TALLINNA TEHNIKAÜLIKOOL
TALLINN UNIVERSITY OF TECHNOLOGY

Department of Materials and Environmental Technology

SPRAY PYROLYSIS OF SNO_2 THIN FILMS FOR PHOTOVOLTAIC APPLICATIONS.

SNO_2 OHUKESED KILED PIHUSTUSSADESTUSE MEETODIL RAKENDAMISEKS PAIKESEPATAREIDES.

MASTER THESIS

Student: Nwaokolo Nwadialor Vivian

Student code 172622 KAYM

Supervisor: Atanas Katerski

Tallinn, 2019

AUTHOR'S DECLARATION

Hereby, I declare, that I have written this thesis independently.
No academic degree has been applied for based on this material. All works, major viewpoints and data of the other authors used in this thesis have been referenced.

".....” 2019

Author: Nwaokolo Nwadialor Vivian

/signature /

Thesis is in accordance with terms and requirements

".....” 2019

Supervisor: Dr Atanas Katerski

/signature/

Accepted for defence

".....”.....2019

Chairman of theses defence commission: .....

/name and signature/

Department of Materials Science.

THESIS TASK

Student: Nwaokolo Vivian, 172622 KAYM (name, student code)

Study programme: KAYM09/09 Materials and Processes for Sustainable Energetics (code and title)

Main Specialty: Materials for sustainable energetics

Supervisor: Researcher, Dr Atanas Katerski, +372 55593056 (position, name, phone)

Thesis topic:

(in English) *Spray pyrolysis of SnO_2 thin films for photovoltaic applications.*

(in Estonian) *SnO_2 ohukesed kiled pihustussadestuse meetodil rakendamiseks paikesepatareides.*

Thesis main objectives:

1. To deposit SnO_2 thin films by Ultrasonic spray pyrolysis on glass, ITO, FTO coated glass substrates at different deposition temperature.
2. To analyze the structural, optical and electrical properties of SnO_2 thin films.
3. To study the IV curve of FTO/SnO_2, ITO/SnO_2, SnO_2/TiO_2 substrates.

Thesis tasks and time schedule:

No	Task description	Deadline
1.	To deposit SnO_2 thin films by Ultrasonic spray pyrolysis on glass, ITO, FTO coated glass substrates at different deposition temperature.	15.01
2.	To analyze the structural, optical and electrical properties of SnO_2 thin films.	22.01
3.	To study the IV curve of FTO/SnO_2, ITO/SnO_2, SnO_2/TiO_2 substrates.	24.04

Language: English **Deadline for submission of thesis:** "27" May 2019

Student: …….. ..... "....."....201….
/signature/

Supervisor: …… ..... "....."....201….
/signature/

Consultant: …… ....."....."....201….
/signature/

Terms of thesis closed defense and/or restricted access conditions to be formulated on the reverse side

Contents

PREFACE

The end of my two-year journey has finally borne fruits as I present to you my thesis titled “Spray pyrolysis of tin iv oxide for photovoltaic applications”. In this work, we studied the electrical, structural and optical properties of SnO_2 deposited by spray pyrolysis for photovoltaic applications. SnO_2 thin films were synthesized by ultrasonic spray pyrolysis (USP) onto glass, FTO and ITO substrates at various deposition temperatures (between 300 and 500 °C) using anhydrous $SnCl_4 \cdot 4H_2O$ as a precursor. The films were investigated for structural, optical and electrical properties using X-ray diffraction (XRD), UV-VIS NIR spectrophotometry, hot probe and I-V measurement respectively. All the films display high transmittance in the visible region with average transmittance varying from 75 to 85 %. XRD analysis showed the polycrystalline nature of our samples. Crystallite size increased from 1.6 nm to 36 nm with increasing deposition temperature. Resistivity and sheet resistance decreased from $1.2.10^{+1}$ to $6.2.10^{-3}$ Ohmcm and $1.2.10^{+6}$ to $6.2.\ 10^{+2}$ ohmcm^2 respectively with increasing temperature. This work has been meticulously written to fulfil the graduation requirements of the Masters of Engineering Degree in Materials and Sustainable Energetics Programme at Tallinn University of Technology, Estonia.

I would like to thank everyone who supported me during my master’s degree journey at Tallinn University of Technology. My first appreciation goes to the Almighty benign God in his infinite mercy for his grace and strength to see me through during trying times. My parents who have been incredibly supportive and my sister Anita who is my guardian angel. My deepest appreciation goes to my Supervisor, Dr. Atanas Katerski, who helped me with his professional expertise and suggestions. Above all, he never gave up on me, his patience and teaching skills was impeccable, I couldn’t have done this all alone without him. Also, my sincere gratitude also goes to the Estonian government and Tallinn University of Technology for supporting my studies and research through the tuition waiver, Dora, Specialty scholarship and Performance scholarships. Those grants were invaluable towards the successful completion of my studies. I am grateful to the course Director, Dr Sergei Bereznev, and all the members of the laboratory of thin film chemical technology at Tallinn University of Technology for their support. Finally, I want to appreciate all my friends, family members and classmates who has supported me throughout my stay in Estonia.

This work is financially supported by the Estonian Ministry of Education and Research projects IUT 19-4 and by the European Union through the European Regional Development Fund “Centre of Excellence” project TK141: “Advanced materials and high-technology devices for sustainable energetics, sensorics and nanoelectronics”.
understanding and support during the phase of my project.

List of abbreviations and symbols

A	absorbance
CSP	chemical spray pyrolysis
Cu	copper
CVD	chemical vapor deposition
D	thickness
E_g	band gap energy
FF	Fill factor
ITO	indium doped tin oxide
J_{SC}	Short Circuit Current
HCl	Hydrochloric acid
PV	Photovoltaics
T	Transmission
SnO_2	tin iv oxide
USP	ultrasonic spray pyrolysis
UV	Ultraviolet
V_{oc}	Open circuit voltage
XRD	x-ray diffraction
α	absorption coefficient

1. INTRODUCTION

Conventional energy sources based on oil, coal, and natural gas have proven to be highly effective drivers of economic progress. However, with the rapid depletion of conventional energy sources, increasing energy demand, and the urgent need for environmental protection there is a call for efficient and environmentally friendly energy systems [1]. The utilization of renewable energy is widely considered as a promising alternative to conventional fossil fuel system and therefore draws more and more attention [2]. There are many forms of renewable energy. Wind and hydroelectric power are the direct result of differential heating of the Earth's surface which leads to air moving about (wind) and precipitation forming as the air is lifted. Solar energy is the direct conversion of sunlight using panels or collectors. Biomass energy is stored sunlight contained in plants. Other renewable energies that do not depend on sunlight are geothermal energy, which is a result of radioactive decay in the crust combined with the original heat of accreting the Earth, and tidal energy, which is a conversion of gravitational energy [2].

Since environmental protection concerns are increasing, both clean fuel technologies and new energies are being intensively pursued and investigated, it is clear that future growth in the energy sector is primarily in the new regime of renewable. Therefore, shifting to renewable energy can help us meet the dual goals of reducing greenhouse gas emissions, thereby limiting future extreme weather and climate impacts, and ensuring reliable, timely, and cost-efficient delivery of energy [3]. The use of solar energy is just one of the green initiatives presented as a solution to the above-mentioned issue. As with any good solution, there has to be a compromise between the efficiency, safety, materials and production costs. The use of non-toxic, earth-abundant materials produced by simple and cost-effective methods can help increase the market share of Renewables.

Solar cells operate on the principle of photovoltaic effect. A semiconductor is used as a light absorber to convert photons from sunlight into an electron-hole pair (Photocurrent generation). The holes and electrons are then separated by the device structure. Electrons migrate to the negative terminals while the holes move to the positive terminals thus producing electric power. Charge separation inside the solar cells leads to the generation of a photovoltage [11]. Photovoltaic (PV) is a promising technology which can be easily installed without affecting neither the landscape nor the natural environment if directly integrated into building. One of the technological key points is the transparent conductive films (TCFs) used for front contact, barrier layer or intermediate reflector [4, 5]. TCFs can be fabricated from both inorganic and organic materials. Inorganic films typically are made up of a layer of transparent conducting oxide (TCO), generally in the form of indium tin oxide (ITO), fluorine doped tin oxide (FTO) and doped zinc oxide usually aluminum doped zinc oxide ZnO:Al (AZO). Organic films are being developed using carbon nanotube networks and graphene. High optical transparency and high electrical conductivity are two critical parameters in the choice of electrodes.

Currently, tin-doped indium oxide (ITO) and fluorine-doped tin oxide (FTO) are used as the primary choice for transparent conductive electrodes (TCE) for such applications due to their high electrical conductivity and optical transparency [4, 6,7].

In the last two years, undoped Tin dioxide (SnO_2) has gained much attention in the field of photovoltaics and optoelectronics due to its suitable optical properties – high transparency, optical bandgap (3.6 eV), n-type semiconductor, electron mobility more than 100 $cm^2V^{-1}s^{-1}$ [APL Mater. 3, 076107 (2015)] useful structure, abundance, mechanical hardness, thermal and chemical stability [8, 9]. SnO_2 have a refractive index of about 1. Due to the suitable properties of SnO_2, the thin films can be used as a window layer in solar cells [10]. These films act as a window for light to pass through to the absorber beneath (where carrier generation occurs), as an ohmic contact for carrier transport out of the photovoltaic. This type of thin film of metal oxides of binary compound without any intentional impurity doping has been developed [4].

In this study, we are looking at the various possibilities of using undoped SnO_2 to improve our glass/ITO/TiO_2/absorber/back contact solar cell stack. One of such possibilities is the use of SnO_2 thin films in the window layer (TiO_2) owing to its better optical properties or as an intermediate buffer layer between the TCO/TiO_2 layer of our solar cell [11]. This is because the conductivity of SnO_2 can be managed. Furthermore, due its useful band structure, high transmittance and stability, they could be used to replace component parts or act as a buffer layer between the front contact electron transport material (ETM) or between the ETM and absorber [12,13]. A broad range of studies has been done in the implementation of SnO_2 thin polycrystalline films in Perovskite solar cells (PSC) [12,13,14,15]. Xiong et al noted a higher efficiency of 20.79% [12]. Hagfeldt and co-workers developed a chemical bath post-treatment SnO_2 PSCs that yielded efficiencies of close to 21%. An impressive certified record efficiency of 20.9% has been achieved by You and co-workers with SnO_2 nanoparticle planar PSCs. This feat is the reason behind our intention to use SnO_2 to improve our solar cell configuration.

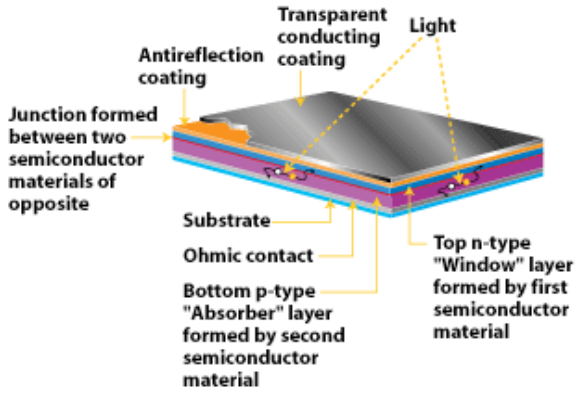

Figure 1. Cross section of a solar cell [16]

Various types of chemical techniques have been used for the deposition of SnO_2 such as chemical spray pyrolysis (CSP) [9, 13, 17] and sol-gel method [18]. D. Jadsadapattarakul et al reported the microstructure of SnO_2 thin films deposited by ultrasonic spray pyrolysis technique [19]. Sehrish et al investigated the photovoltaic properties of SnO_2 using sol-gel method [18] while S. Palanichamy et al have reported on the physical properties of SnO_2 thin films using nebulised spray pyrolysis [17] at different temperatures. Ultrasonic chemical spray pyrolysis (USP) method is a well-developed and economically viable method for depositing uniform thin films over large area [20]. USP is a processing technique being considered in research to prepare thin and thick films, ceramic coatings, and powders. Unlike many other film deposition techniques, it represents a very simple and relatively cost-effective processing method (especially regarding equipment costs). It offers an extremely easy technique for preparing films of any composition. The aim of this study is to successfully deposit uniform transparent SnO_2 thin films by USP method onto different substrates (glass and glass/ITO) which are useful for photovoltaic applications and to investigate their structural and electrical properties. This thesis is divided into three main chapters. Following the introduction, the theoretical part describes a general overview of SnO_2 applications, deposition methods, effects of external factors, and properties. The experimental part briefly describes characterization techniques while the third part is analyses the results and discussions of the properties of SnO_2 thin films.

1.1 AIM AND OBJECTIVE OF STUDY.

1) To deposit undoped SnO_2 thin films using ultrasonic spray pyrolysis method.
2) To study the electrical, structural and optical properties of Undoped SnO_2 thin films.
3) To obtain high transparency and homogeneity of Undoped SnO_2 thin films.
4) To prove the intermediate conductivity around of SnO_2 thin film.

2. BACKGROUND AND LITERATURE REVIEW

2.0 TIN IV OXIDE

Metal oxides are the basis of modern diverse smart and functional materials and devices because physical and chemical properties of these oxides can be tuned. Metal oxides SnO_2, ZnO, In_2O_3, and CdO are wide-bandgap *n*-type semiconductors. They belong to a class of transparent conductive oxides due to a number of unique functional properties, of which the most important are the electrical conductivity, the visibility in a wide spectral range, and high reactivity of the surface. Tin dioxide (stannic oxide) is the inorganic compound with the formula SnO_2. The mineral form of SnO_2 is called cassiterite, and this is the main ore of tin. They are generally regarded as an oxygen deficient n-type oxide and have a wide range of applications, including transparent electrodes in devices, gas sensors, and transparent heat- reflecting films [23], [24], [25]. SnO_2 semiconductors have been studied widely owing to their relatively large optical of 3.6 eV and excellent transparency of >85% [26].

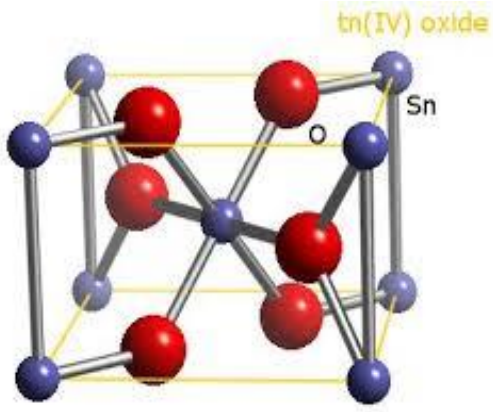

Figure 2. The unit cell of the rutile structure (27).

SnO_2 conforms to the O=Sn=O structure. Interestingly, the simultaneous occurrence of transparency and conductivity of SnO_2 is a unique feature among the Group-IV elements of the periodic table [28]. For example, its superior optical transparency is suitable for optically passive component in number of devices [28, 29]. The study of SnO_2 is triggered by its impressive range of applications in solar cells [28, 30]. The key for understanding various aspects of SnO_2 is its surface properties which eventually are governed by the dual valency of Sn. The dual valency facilitates a reversible transformation of the surface composition from stoichiometric surfaces with Sn^{4+} surface cations into a reduced surface with Sn^{2+} surface cations depending on the oxygen chemical potential of the system [28, 31]. Medvedeva et al [32] formulated criteria for the successful combination of high electrical conductivity with complete transparency in the visible range and emphasized the significant correlation between their structural attributes with the electronic and optical properties. In the direct band structure of SnO_2, the top of the valence band mostly consists of O(p) states,

while the bottom of the conduction band has an anti-bonding character arising from the Sn(4s) and O(p) states [28].

2.1 CHARACTERISTICS OF TIN IV OXIDE

SnO_2 is a transparent semiconductor with up to 97% optical transparency in the visible range (for films of thickness 0.1-1 µm), yet having a resistivity of 10^{-4} -10^{6} Ωcm, considerably lower than most semiconductors (10^{-3} - 10^{9} Ωcm). Remarkably, nominally undoped SnO_2 has a carrier density of up to 10^{-20} cm^{-3} which is comparable to that of semimetals (10^{17} -10^{20} cm^{-3}) [33]. Furthermore, SnO_2 possesses several polymorphs such as the rutile-type $CaCl_2$ (Orthorhombic), α-PbO_2-type (Orthorhombic), fluorite-type (Cubic. See Chapter 4.1.1), ZrO_2-type (Orthorhombic phase I) and cotunnite-type (Orthorhombic phase II) structures. Thus, the most important form of naturally occurring SnO_2 is cassiterite (tin oxide mineral), a phase of SnO_2 with the tetragonal rutile structure [28, 34].

Table 1. Crystal properties of SnO_2 [35]

Chemical name	Tin (IV) oxide
Mineral name	Cassiterite
Formula	O_2Sn
Crystal structure	Tetragonal rutile
Bandgap (eV)	3.6
Lattice Constants (nm)	a = 0.474 b =0.319
Density ρ (g cm^{-3})	6.99
a (Å)	4.7380(1)
b (Å)	4.7380(1)
c (Å)	3.1865(2)
α (°)	90
β (°)	90
γ (°)	90
V ($Å^3$)	71.5
Space group	$P4_2/mnm$

2.2 DEPOSITION METHODS FOR THIN FILMS

Thin film can be defined as a thin layer of material, where the thickness is varied from several nanometers to few micrometers. Like all materials, the structure of thin films is divided into amorphous and polycrystalline

structure depending on the preparation conditions as well as the material nature. The properties and versatility of the thin films can be obtained by selecting proper technique of film deposition. Thin film deposition methods can be broadly classified as either chemical or physical methods. The difference between the chemical and physical thin film deposition methods depends upon the method of depositing thin film material on the substrate. It can be summarized as shown in table 2 below:

Table 2. Summary of physical and chemical deposition methods.

Physical deposition	**Chemical deposition**
1. **Evaporation techniques** 1. Vacuum thermal evaporation. 2. Electron beam evaporation. 3. Laser beam evaporation. 4. Arc evaporation. 5. Molecular beam epitaxy. 6. Ion plating evaporation.	1. **Sol-gel technique**
2. **Sputtering techniques** 1. Direct current sputtering (DC sputtering). 3. Radio frequency sputtering (RF sputtering).	2. **Chemical bath deposition**
	3. **Spray pyrolysis technique**
	4. **Plating** 1. Electroplating technique. 2. Electroless deposition.
	Chemical vapor deposition (CVD) 3. Low pressure (LPCVD) 4. Plasma enhanced (PECVD) 5. Atomic layer deposition (ALD)

2.3 CHEMICAL SPRAY PYROLYSIS (CSP)

Chemical spray pyrolysis is a processing technique being considered in research to prepare thin and thick films, ceramic coatings, and powders. Unlike many other film deposition techniques, spray pyrolysis represents a very simple and relatively cost-effective processing method (especially with regard to equipment costs). It offers an extremely easy technique for preparing films of any composition. Spray pyrolysis does not require high-quality substrates or chemicals [36].

Chemical spray pyrolysis is a process in which a thin film is deposited by pulverization of a precursor solution in the form of micron dimension droplets onto a preheated substrate where the precursor salts undergo pyrolysis to form a desired chemical compound as an adherent film from more thermally stable compound and volatile by-products evaporates. This process is especially useful for the thin films deposition of metal oxides [37]. In the CSP method, thin films are synthesized by nebulizing fine droplets of precursor solutions containing metal salts and different additives (acids, complexing agents etc.) onto preheated substrates. The schematic diagram of the spray pyrolysis system is presented in Figure 3. The typical CSP system is composed of an atomizer, which helps to produce aerosols, a solution vessel, a heater, and a temperature controller [38]. Depending on the atomizer type used, the CSP method can be categorized into three modes: pneumatic, ultrasonic and electrostatic [37, 39, 40, 41]. Different parameters such as the deposition temperature, carrier gas, solution spray rate, concentration of starting chemicals in a solution, the distance between a spray nozzle and substrates, nature of the substrates and solvents have been reported to influence the film properties [42].

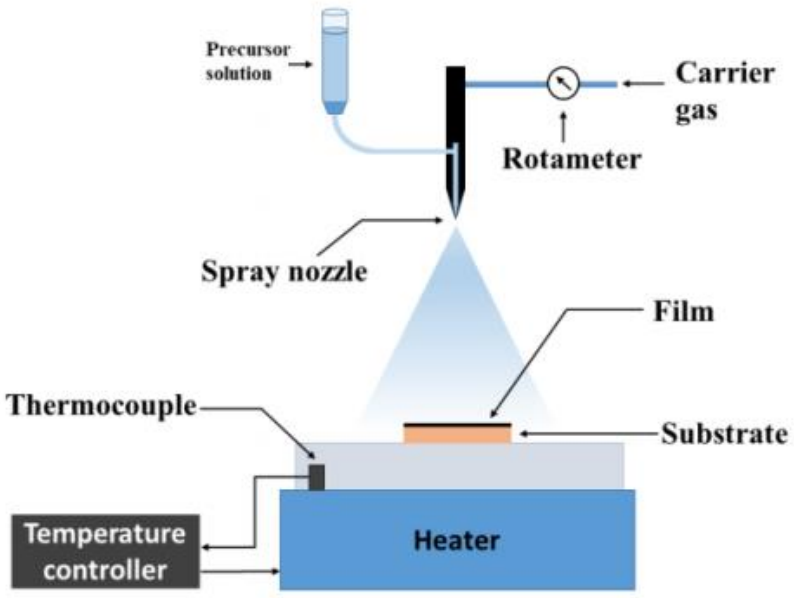

Figure 3. Scheme of the chemical spray pyrolysis system (38)

2.3.1 PNEUMATIC SPRAY PYROLYSIS (PSP)

Pneumatic spray pyrolysis belongs to chemical spray pyrolysis which uses pneumatic nebulizer to generate small droplets for the deposition of thin films. It is convenient and simple to use, inexpensive, absence of vacuum, easy to control the composition and microstructure and can be used for mass production. Despite its advantages, disadvantages include: Difficulties with determination of growth temperature, hard control of aerosol flow rate and film quality may depend on the droplet size and spray nozzle [37, 38].

2.3.2 ULTRASONIC SPRAY PYROLYSIS (USP)

Ultrasonic spray pyrolysis method was used for the deposition of SnO_2 thin film in this study. In the process of USP, ultrasonic atomizers have been used in order to obtain homogeneously distributed micron sized droplets. Generally, the precursor solution is usually vaporized using an ultrasonic atomizer, the generated fine droplets are transported by the carrier gas to the heated substrate. The solvent will vaporize when the droplets approach the substrate and the reactants will diffuse to the substrate to form thin film. USP method is a promising technique, which is considered to be an alternative of chemical vapor deposition and for some cases for Atomic Layer Deposition (ALD). Besides the advantages already mentioned in pneumatic spray pyrolysis, it also has advantages over pneumatic spray pyrolysis which are listed below [37, 43, 44]:

(1) The gas flow rate of USP is independent of the aerosol flow rate.
(2) Easier to control the spray flow and deposit thinner and more homogeneous layer.
(3) The droplet size of the precursor solution is smaller.
(4) The drop size can be decreased by increasing the ultrasonic frequency.
(5) Possibility of high spray rate.
(6) The place of spraying is not over-cooling.

Disadvantages include [37, 43, 44]:

(1) Spray rate is dependent on viscosity of the precursor solution.

2.4 FORMATION OF TIN IV OXIDE BY CHEMICAL SPRAY PYROLYSIS

Generally, in spray pyrolysis, thin films of SnO_2 films are prepared by the reaction:

$$SnCl_4 + 2H_2O \rightleftharpoons SnO_2 + 4HCl \qquad (4.1)$$

If this reaction is completed, the resulting $Sn0_2$ would become an insulator after the completion of the reaction. Since the films obtained by pyrolysis decomposition are conducting, the expected reactions are:

$$2SnCl_4 + 4H_2O \rightleftharpoons SnO_2 + SnO + 7HCl + \frac{1}{2}O_2 + \frac{1}{2}Cl_2 + \frac{1}{2}H_2 + e \qquad (4.2)$$

$$2SnCl_4 + 4H_2O \rightleftharpoons SnO_2 + SnO + 8HCl + \frac{1}{2}O_2 + 2e \qquad (4.3)$$

Alternately, doubly ionized oxygen vacancies predominate in SnO_2 according to the defect reaction:

$$Sn + 2O \rightleftharpoons Sn + 2V_{\ddot{O}} + 4e' + O_2(g) \qquad (4.4)$$

Hence the film contains $SnO_{2-x}(V_O^{\cdot\cdot})_x e'_{2x}$, where x is the deviation from stoichiometry Vo, denotes the doubly ionized oxygen vacancies and e' denoted the electrons, which are needed for charge neutrality on macroscopic scale. These defects are considered to be electron donors. Thus, the conductivity of SnO_2 is due

to oxygen vacancies that result from incomplete oxidation of the film. The properties of tin oxide films depend largely on the preparation conditions. At small distances between substrate and nozzle, the maximum amounts of solution vapour molecules, which emerge from the nozzle, strike directly on the substrate before they get distributed. At sufficiently large distances the substrate receives no coating even after a long spraying time. Vasu et al (1990) reported that substrate nozzle distance is significant in the pyrolytic reaction. At high liquid flow rate and at low substrate temperature the film growth is controlled by the rate at which the reaction proceeds on the substrate [45, 46].

2.5 INFLUENCE OF DEPOSITION PARAMETERS ON THIN FILM PROPERTIES.

This section deals with the influence of the main spray pyrolysis parameters on structure and properties of the deposited films.

2.5.1 Influence of Temperature

Chemical spray pyrolysis involves many processes occurring either simultaneously or sequentially. The most important of these are precursor decomposition, aerosol generation and transport, solvent and by-products evaporation and droplet impact with consecutive spreading. The deposition temperature is involved in all mentioned processes, except in the aerosol generation. Consequently, the substrate surface temperature is the main parameter that determines the film morphology and properties [47]. In this study, we can see in Chapter 4 how increase in temperature affected electrical, optical and structural properties.

For thermal-decomposition (pyrolysis) of the solid precursor (after evaporation of the solvent), if temperature is not enough for pyrolysis, a layer/film from solid precursor will be obtained and desired compound will be not formed. Also, when we have enough temperature for pyrolysis of the precursor salt, the by-products are evaporated away from the system. The remaining product is more thermally stable and desired. Variations in temperature is often used to change the crystallinity of the film. Lastly, if the temperature is so high that the solvent is evaporated before droplets reach the surface of the sample, an unwanted porous layer is formed.

2.5.2 Influence of Precursor Solution

The precursor solution is the second important process variable. Solvent, type of salt, concentration of salt, and additives influence the physical and chemical properties of the precursor solution. Therefore, structure and properties of a deposited film can be tailored by changing composition of precursor solution. Chen et al. have shown that the morphology of the thin films can be changed considerably by adding additives to the precursor solutions [48]. Furthermore, Vasu et al observed that the growth rate of SnO_2 films prepared from $SnCl_4 \cdot 5H_2O$ was higher and their resistance lower in comparison with those prepared from anhydrous $SnCl_4$. The authors suggested that under identical conditions, the droplets containing $SnCl_4 \cdot 5H_2O$ require more

thermal energy to form SnO_2 than those containing $SnCl_4$. Thus, the water molecules seemed to influence the reaction kinetics, particularly the growth rate of the films [47, 49].

2.6 APPLICATIONS OF TIN IV OXIDE

The surface and materials properties of SnO_2 have three major applications. These applications are (i) as a transparent conducting oxide (TCO), (ii) as an oxidation catalyst, and (iii) as a solid-state gas sensing material.

2.6.1. Transparent Conductors

SnO_2 belongs to the important family of oxide materials that combine low electrical resistance with high optical transparency in the visible range of the electromagnetic spectrum. These properties are sought in a number of applications; notably as electrode materials in solar cells, light emitting diodes, flat panel displays, and other optoelectronic devices where an electric contact needs to be made without obstructing photons from either entering or escaping the optical active area and in transparent electronics such as transparent field effect transistors [50], [51], [52], [53]. Another property of SnO_2 and other TCOs is that although they are transparent in the visible they are highly reflective for infrared light. This property is responsible for today's dominant use of SnO_2 as an energy conserving material. SnO_2-coated architectural windows, for instance, allow transmitting light but keeping the heat out or in the building depending on the climate region. More sophisticated architectural windows, so-called smart windows, rely on TCOs to electrically contact electrochromic films that are changing their coloring and transparency by applying a voltage across the films [54], [55], [56].

There is a large number of TCOs, the most commonly known ones are the binary systems, i.e. SnO_2, ZnO, In_2O_3 (better known as ITO if doped with Sn), Ga_2O3, and CdO [57], [58]. The coexistence of high electrical conductivity and optical transparency of TCOs are due to the combination of several properties of the band structure of these materials. These can be summarized in a simplified form as follows: (i) TCOs exhibit a wide optical band gap prohibiting interband transitions in the visible range. (ii) Intrinsic dopants (oxygen deficiency) or impurity dopants donate electrons into the conduction band. This causes a light effective mass of conduction electrons (in contrast to the heavy holes in these materials) and results in a uniform distribution of the electron charge density and hence relative low scattering. These effects contribute to the high mobility of the conduction electrons. (iv) A large internal gap in the conduction band prohibits inter-conduction-band adsorption of photons in the visible range [59].

2.6.2. Heterogenous Catalysts

Many oxides mainly act as a support material for dispersed metal catalysts; tin oxide, however, is an oxidation catalyst in its own right. Tin-oxide based catalysts exhibit good activity towards CO/O2 and CO/NO reactions [60]. The activity and selectivity of tin-oxide catalysts can be substantially improved by incorporation of

heteroelements [61]. For instance the addition of copper, palladium [62], [63], [64], chromium and antimony increases the total oxidation of carbon monoxide and hydrocarbons. The role of many of these additives is not fully understood. Most of the additives are oxidized during operation conditions of the catalyst. A strong synergetic effect between the additive and SnO_2 is usually proposed that is manifesting itself in several ways. Special active sites may be stabilized at the interface between the additive and SnO_2. For example, Mo^{5+} has been identified in MoO_3 catalysts supported on SnO_2. It was suggested that these Mo^{5+} sites play an important role in methanol and ethanol oxidation to formaldehyde and acetaldehyde or acetic acid, respectively [65], [66].

In most cases the additives form clusters supported on SnO_2, for antimony, however, it is suggested that antimony oxide forms a solid solution with SnO_2 with a strong surface segregation of Sb. Thus Sb^{3+} surface species may be the active sites. The combination of the various electronic effects on semiconducting oxides and the creation of special sites make it difficult to find a fundamental description and understanding of the role of additives; even if the catalysts were fully characterized. Dynamic changes of the catalyst during operation adds to the challenge of understanding complex heterogenous catalysts. The probably best-known example, where decades of research have not yet been able to completely explain the synergy between an oxide and a metal is the hugely important methanol synthesis catalyst Cu/ZnO. Since ZnO shares a similar electronic structure with SnO_2 that gives rise to similar applications (gas sensing, and transparent conductor) some of the lessons learned from studying ZnO may be cautiously applied to SnO_2 [59].

2.6.3 Solid state gas sensors

Materials that change their properties depending on the ambient gas can be utilized as gas sensing materials. Usually changes in the electrical conductance in response to environmental gases are monitored. Many metal oxides are suitable for detecting combustible, reducing, or oxidizing gases. For instance, all the following oxides show a gas response in their conductivity: TiO_2, Cr_2O_3, Mn_2O_3, Co_3O_4, NiO, CuO, CdO, MgO, SrO, BaO, In_2O_3, WO_3, V_2O_3, Fe_2O_3, GeO_2, Nb_2O_5, MoO_3, Ta_2O_5, La_2O_3, CeO_2, Nd_2O_3. However, the most commonly used gas sensing materials are ZnO and SnO_2 [67]. Pure oxides exhibit gas sensing properties by themselves. In practice additives are often included to increase the sensitivity and selectivity to certain gases. Before we discuss the influence of additives on the gas response we describe the fundamental gas sensing mechanism of pure SnO_2 in the next subsection [59].

2.7. CHARACTERIZATION TECHNIQUES FOR THIN FILMS.

Various techniques are used for the characterization of thin film properties. In this work we investigated the crystallographic properties of SnO_2 thin films by means of X-ray diffraction (XRD). For the analysis of optical characteristics, a UV-vis spectroscopy was used. Finally, for the investigation of electrical properties of SnO_2 thin films Hall effect and van der Pauw techniques were applied. For the fast determination of conductivity type, hot-probe method was used.

2.7.1. XRD

XRD measurements are conducted to determine phase composition and crystallographic properties of thin films. On the basis of XRD measurements lays the classical electromagnetic theory when an electron is oscillating in alternating electromagnetic field with the same frequency as the field. When an X-ray beam hits the atom, electrons of that atom will oscillate in the frequency of the beam. An accelerated charge emits electromagnetic radiation. In most cases the emitted radiation interferes destructively, however in the right angle of radiation the emitted radiation coincides and leave the crystal. Diffraction of X-rays is described by Bragg's equation [4.5].

$$n\lambda=2d\cdot sin\theta \qquad [4.5]$$

where λ is X-ray wavelength, d is interplanar distance, θ is angle of incidence with lattice plane and n is integer. X-rays with constant wavelength are radiated towards crystal lattice, radiation reflects from lattice atoms illustrated in Figure 6 which is captured by detector [68, 69].

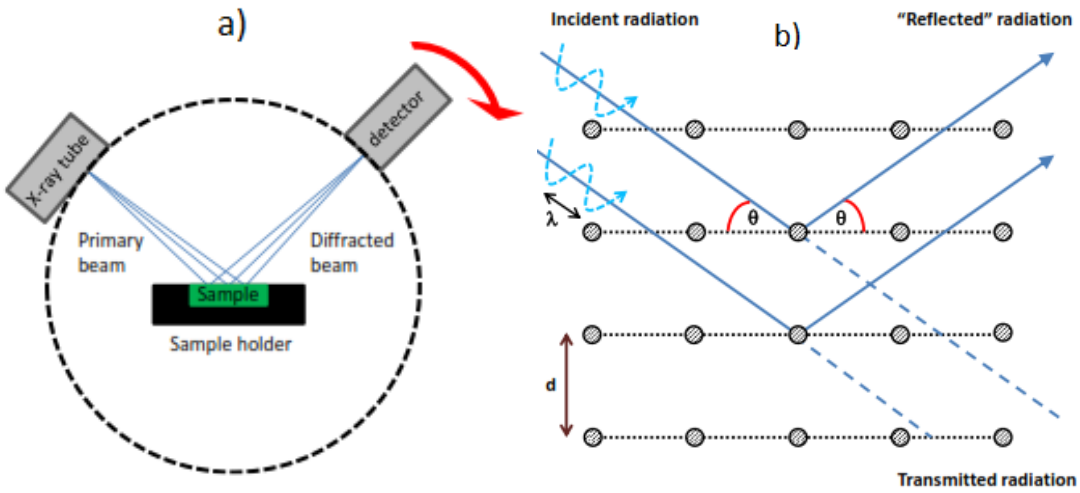

Figure 4. a) Scheme of XRD measurement and b) Bragg's geometry of X-ray reflection [68].

The intensity of detected radiation is plotted against 2θ. As it is seen in Figure 4, the angle of radiation is varied to find angles where Bragg's equation [4.5] is satisfied. These angles will generate diffraction peaks in the XRD pattern and these peaks can be compared with previous experimental data giving us information of phase composition, lattice parameters and crystallites orientation [68].

2.7.2 UV-VIS SPECTROSCOPY

UV-vis spectrometry is applied to describe thin film optical characteristics such as transmittance, reflectance and absorbance which also allow determining the thickness, the absorption coefficient and the band gap of

the film. Transmittance and reflectance spectra are measured inside an integrated sphere which scheme can be seen in Figure 5.

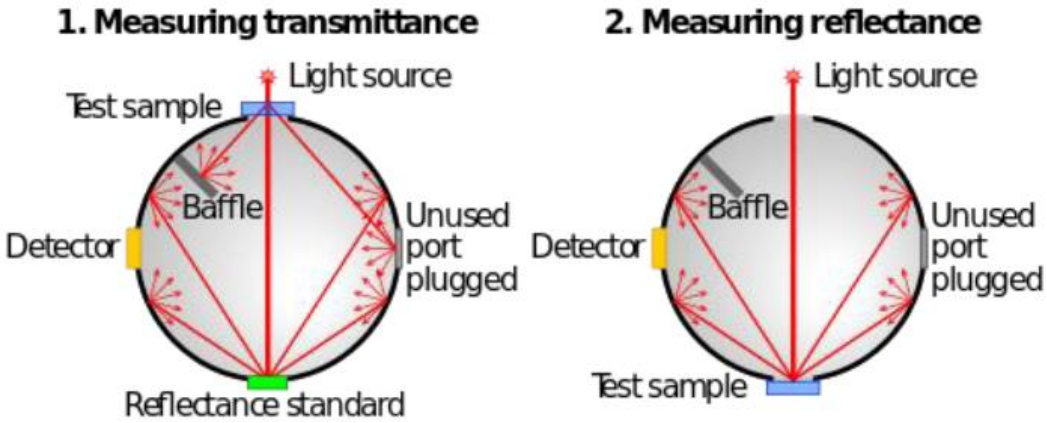

Figure 5. Schemes of transmittance and reflectance modes in the UV-vis spectrometry [68].

Transmittance and reflectance spectra are obtained by dividing transmitted or reflected light to the incident light. Based on these spectra the absorption coefficient, α, can be calculated by means of equation [4.6].

$$\frac{T}{100-R} = e^{-\alpha d} \qquad [4.6]$$

where d is the thickness of the film.

The optical band gap is evaluated from the Tauc's relation between Eg and derived absorption coefficient. See equation below:

$$(\alpha h\nu)^n = (h\nu - E_g) \qquad [4.7]$$

where A is a constant, h is Planck's constant, ν is light frequency. The value of n number is 2 for direct transitions and 0.5 for indirect transitions. The linear part of a plot of $(\alpha h\nu)^2$ against photon energy (hν) is extrapolated to x-axis, giving the value of [E_g] [68, 70].

2.7.3 HALL EFFECT AND VAN DER PAUW

Van der Pauw or four-point probe technique can be used to measure sheet resistance of a film. Knowing thickness of the sample the electrical resistivity can be also calculated. For the measurement procedure four points are chosen in the corners of a square in a fashion shown in Figure 6.

The measurement is based on a relation seen in equation [4.8]

$$exp\left(\frac{-\pi d}{\rho} R_A\right) + exp\left(\frac{-\pi d}{\rho} R_B\right) = 1 \qquad [4.8]$$

where d is the thickness of the thin film, ρ is the resistivity of the material, whereas R_A and R_B are sheet resistances Figure 8 [68, 71].

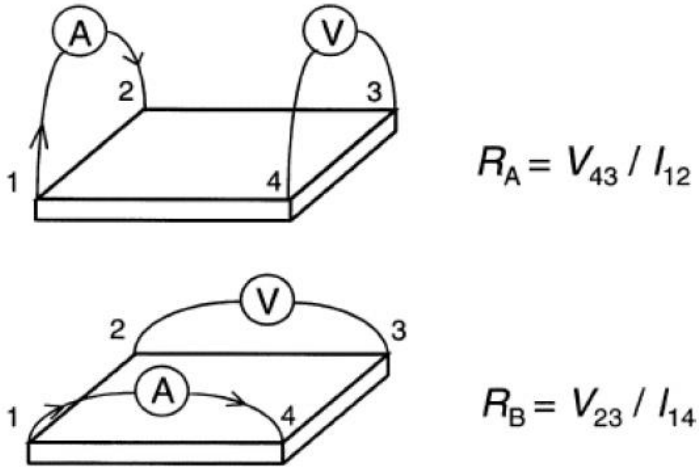

Figure 6. Four-point probe contact illustration. *[68]*

The Hall effect is due to the nature of the current in a conductor which consists of the moving charge carriers, typically electrons, holes, ions or all three move in a straight line. When a magnetic field is present, these charges experience a force, called the Lorentz force, which curve the paths of charge carriers in a manner that moving charges accumulate on one face of the material in Figure 9. This leaves equal and opposite charges exposed on the other face, where there is a scarcity of mobile charges establishing and electric field [68].

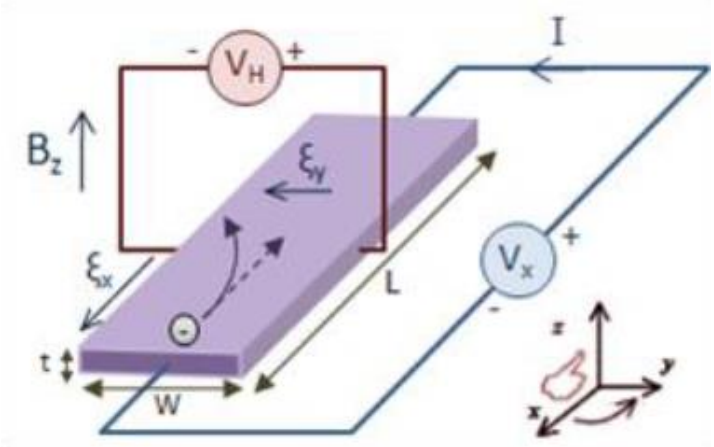

Figure 7. Scheme of Hall measurement. *[68]*

The Hall effect is very useful as a means to measure either the carrier density or the magnetic field.

2.8 CURRENT VOLTAGE CHARACTERISTICS OF SOLAR CELLS

To characterize a solar cell, standard device performance parameters such as open circuit voltage (V_{OC}), short circuit current density (J_{SC}), fill factor (FF) and efficiency are used. These parameters are extracted from the graphical representation of Schockley diode equation [4.9]

$$J = J_0 \left(e^{\frac{qV}{AkT}} - 1 \right) \qquad [4.9]$$

where J is the diode current density, J_0 is the reverse saturation current density, q is the electron charge, V is the voltage, A is the diode ideality factor, k is Boltzmann's constant, and T is the temperature. When device is placed under a light source a light generated current density term (J_L) is added to the equation [5.0].

$$J = J_0\left(e^{\frac{qV}{AkT}} - 1\right) - J_L \qquad [5.0]$$

J-V curves for an ideal device in dark or under illumination are represented in Figure 8 [68,73]. Based on these dependencies the photovoltaic parameters of the solar cell can be determined. J_{SC} is the current generated by the device under no applied bias (V=0) and is determined as the y-intercept of the light J-V curve in Figure 8. V_{OC} is defined as the applied bias at which n current flows through the device and is determined from the x-intercept of the light J-V curve in Figure 8. The V_{OC} can be also determined from equation [5.0] by setting the condition that J=0.

$$V_{OC} = \frac{nkT}{q} ln\left(\frac{I_L}{I_0} + 1\right) \qquad [5.1]$$

It is clear that V_{OC} is a function of dark as well as light generated current density terms equation [5.1]. The fill factor is a measure of the "squareness" of the curve with higher values tending towards a square response and lower values tending towards a straight line. The fill factor is defined as a ratio of the size of the maximum power rectangle to the rectangle formed by the product of the short current density and open circuit voltage, which can be calculated with the following equation:

$$FF = \frac{Pmp}{JscVoc} = \frac{JmpVmp}{JscVoc} \qquad [5.2]$$

Device efficiency (η) is defined as the ratio of the maximum power generated by the device (P_{mp}), to the power of the radiation incident upon it (P_s) and is calculated as follows [68].:

$$\eta = \frac{P_{MP}}{P_{IN}} = \frac{(V_{OC}J_{SC}FF)}{P_{IN}} \qquad [5.3]$$

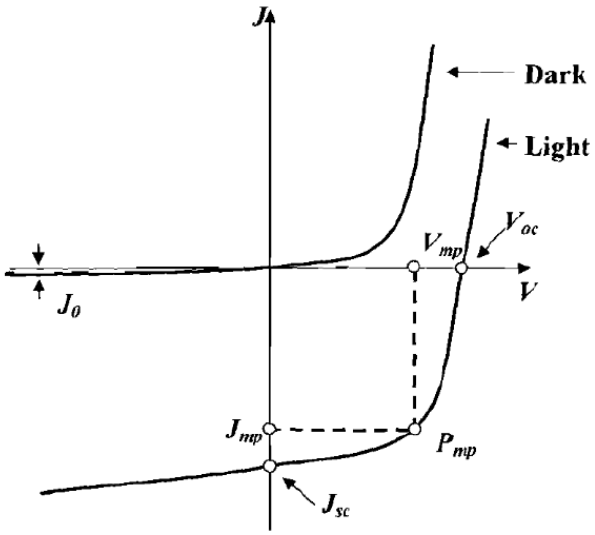

Figure 8. Ideal diode J-V curves for measurement in the dark and under illumination [68].

2.9 SUMMARY OF LITERATURE REVIEW

Chapter two can be summarized as follows:

1) Tin dioxide (stannic oxide) is the inorganic compound with the formula SnO_2. The mineral form of SnO_2 is called cassiterite, and this is the main ore of tin. They are generally regarded as an oxygen deficient n-type oxide and have a wide range of applications, including transparent electrodes in devices, gas sensors, and transparent heat- reflecting films. SnO_2 semiconductors have been studied widely owing to their relatively large optical of 3.6 eV and excellent transparency of >85% .
2) Spray pyrolysis is a processing technique being considered in research to prepare thin and thick films, ceramic coatings, and powders. Unlike many other film deposition techniques, spray pyrolysis represents a very simple and relatively cost-effective processing method (especially with regard to equipment costs). It offers an extremely easy technique for preparing films of any composition. Spray pyrolysis does not require high-quality substrates or chemicals.
3) Temperature and Precursor solution influences the deposition of thin films.
4) There are various applications of tin iv oxide, but the three major applications are as a transparent conducting oxide, as an oxidation catalyst and solid-state gas sensing material.
5) There are various characterization of thin films but for this paper, we would be using X-ray diffraction, UV-vis spectroscopy, Hall effect and van der Pauw.

3. EXPERIMENTAL

3.1 Cleaning of Substrates

Soda-lime glass and glass/ITO substrates (10 x 20 x 1 mm) dimensions was washed with soap solution and rinsed in distilled water. The substrates was then placed in ethanol and ultrasonically cleaned in ultrasonic bath for 30 minutes. After proper cleaning, the substrates were dried by compressed air and ready for the spray deposition.

3.1.1. Chemicals

The Chemicals used for deposition of SnO_2 films are listed in table 3

Table 3. Precursors used for the preparation of spray solution.

Deposited Materials	**Precursor**	**Formula**	**Company**	**Purity**
SnO_2 thin films	Tin (IV) chloride hydrate	$SnCl_4.4H_20$	Sigma-Aldridge	≥98%
	Pure water	H_2O	Laboratory	>18 MΩ·cm
	Hydrochloric acid	HCl	Sigma-Aldridge	≥98%

3.1.2 Preparation of Spray Solution

3.31g of tin (iv) chloride was added to 100 ml of pure water (with more than 18 MΩ·cm resistivity) to make 0.1M solution. Few drops of hydrochloric acid was added to the solution to prevent hydrolysis (Note: Reaction of hydrolysis of $SnCl_4$, $SnCl_4 + 4H_2O \rightleftarrows Sn(OH)_4 + 4HCl$) and the solution was stirred for homogeneity. The deposition of SnO_2 thin film was immediately started after the solution was ready. For this experiment, thin films are defined as having 50-150 nm thickness.

3.2 USP apparatus and parameters

The setup of ultrasonic spray pyrolysis is presented in Figure 9. This spray system mainly consists of an ultrasonic generator, air compressor, heater, temperature controller, air flow meter, pipe for transportation of aerosol. The temperature controller can control the temperature of the substrate.

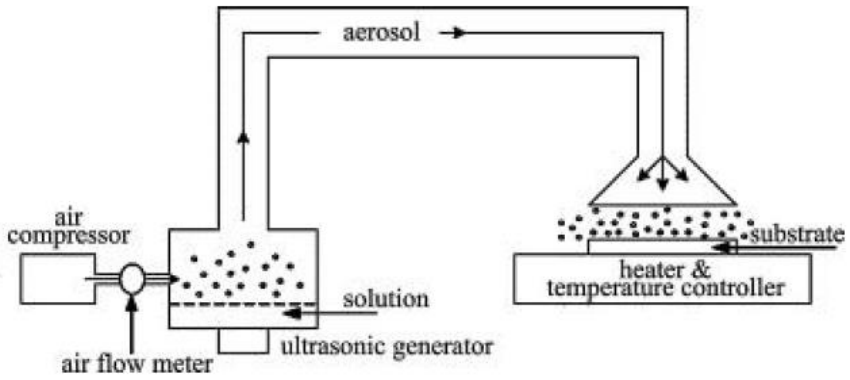

Figure 9. Experimental setup for ultrasonic spray pyrolysis [37, 72].

3.3 Deposition of SnO_2 thin films.

Before deposition, the substrate was put on the center of the heater for a while in order for it to reach the required temperature. The deposition temperature was set on a temperature controller which controls the heater. The solution was then poured into the ultrasonic generator. The carrier gas flow rate was set at 5 L/min for 5 and 10 minutes. After the heater reached the desired temperature, the ultrasonic generator was plugged in to generate aerosol.

Finally, the air controller was switched on and spray deposition started. Deposition parameters of SnO_2 thin films on different substrates are listed in Table 4.

Table 4. Deposition parameters of the SnO_2 thin films by ultrasonic spray pyrolysis method using 5 L/min carrier gas flow rate.

Substrate	**Condition**	**Substrate temperature (°C)**
Glass/SnO_2	0.1M/L SnO_2 5 and 10 minutes	300
ITO/SnO_2		400
Glass/SnO_2		500
ITO/SnO_2		300
Glass/SnO_2		400
ITO/SnO_2		500

3.4. Preparation of solar cell

The structure of prepared solar cells were as follows: glass/ITO/SnO_2/TiO_2/Sb_2Se_3/C. For solar cells preparation was used commercial glass/ITO substrates with sheet resistance less than 12 Ω/□. TiO_2 films were deposited by spray using titanium tetra iso-propoxide and acetil acetonate dissolved in ethanol. As

absorber material was used vacuum thermal evaporated Sb_2Se_3 at room temperature. Graphite paste was used as a back electrode.

3.5. Characterization methods

3.5.1. X-ray diffraction

The structural properties of the samples deposited onto Soda-lime glass and glass/ITO substrates were investigated by X-ray diffraction (XRD) using ULTIMA IV Rigaku D/Max 2500 diffractometer using a Cu Ka radiation (λ=1.5406 Å, 40 kV at 40 mA). The measurements were performed in 2 theta configurations with scan range of 20-60 ° with a step of 0.02 ° and a scanning speed of 5 °/min.

XRD measurements were carried out with the help of Erki Kärber and Atanas Katerski.

3.5.2. UV-visible Spectroscopy

The total transmittance and total reflectance of SnO_2 thin films on Soda-lime glass and glass/ITO substrates were measured by Jasco V-670 spectrophotometer with spectral range between 250 and 1500 nm. The optical properties were investigated. The film thickness was calculated by Spectra manager program using interference fringes from the spectrum of total transmittance and total reflectance.

3.5.3. Hot probe method

A hot point probe is a method of determining quickly whether a semiconductor sample is n (negative) type or p (positive) type of conductivity. A voltmeter was attached to glass/SnO_2 and glass/ITO/SnO_2 substrates, and a heat source, such as a soldering iron, was placed on one of the leads. n type conductivity was observed.

3.5.4 Electrical Measurements

Four probe method.

The resistivity, charge carrier concentration and mobility were measured at room temperature using MMR's Variable Temperature Hall System and a Hall and van der Pauw controller H-50. The contact material (indium) for electrical measurements was evaporated through mica mask, which had openings for four-point contact van der Pauw geometry.

Current-voltage measurements.

Current-Voltage (I-V) measurement was performed to investigate the electrical properties of TiO_2 thin film on glass and Si substrates and the properties of SnO_2 hybrid solar cells. The Autolab PGSTAT 30 system was used for measuring of I-V curves of the films. The software Frequency response analyzer was used to obtain the data. The I-V measurements were carried out with the help of Research Scientist, Atanas Katerski. The Current-Voltage (I-V) measurement was also performed for the SnO_2 solar cells. The SnO_2 solar cells were placed under simulated sunlight DC measurements were carried out to get the I-V curve. The out-put properties of the SnO_2 solar cells were characterized by recording the I-V curves under simulated sunlight (100 mW/cm^2). This measurement was carried out with the help of Research Scientist, Atanas Katerski.

CHAPTER FOUR

4.1 RESULTS AND DISCUSSIONS

4.1.1 Structural Analysis of SnO_2 thin films.

The XRD diffraction pattern of SnO_2 thin films deposited for 5 min and 10 min are shown in Figure 10 below. According to XRD pattern, cassiterite (ICDD: 01-077-0448) was detected which revealed the polycrystalline nature of the film having a tetragonal structure. Although, a cubic SnO_2 (ICDD: 01-071-5329. See Chapter 2) with orientation (111) was also detected for both graphs. No reflection connected to an additional phase was noticed. The film at Ts = 300 °C crystallize in cubic polymorph. Only (111) direction of cubic SnO_2 was detected. At 500 °C, XRD shows well defined peaks of (110), (101), (200), (211), (220), (310), (112), (321). Two polymorphs, cubic and orthorhombic SnO_2 were detected at both 400 °C and 500 °C.

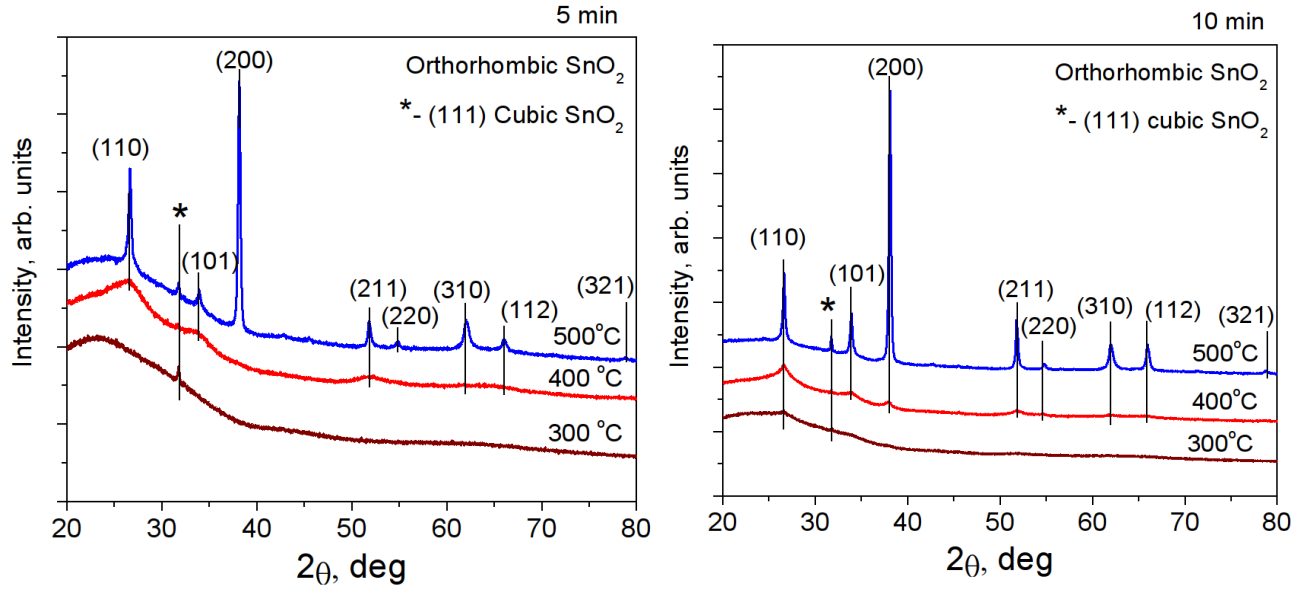

a) ***b)***

Figure. 10. XRD plot of sprayed SnO_2 thin films deposited onto glass substrate (a) for 5min (b) for 10min.

The plane (200) appears and was dominant at 500 °C. Similar observation of orientation was reported by Maio et al [73]. Furthermore, a report produced by S. Palanichamy revealed the polycrystalline nature of the SnO_2 thin films and an increase in crystallinity with substrate temperature [9].

The crystallite size of the SnO_2 thin films deposited glass/SnO_2 substrates and annealed at different temperatures was calculated by applying the Scherrer's formula. The equation is below:

$$d = \frac{k\lambda}{B\left(\frac{1}{2}\right)cos(\theta)} \qquad [5.4]$$

Where

d – crystallite size, nm,

k – Shape constant, 0.9,

λ=1.54 Å is the wavelength of CuKα radiation, nm,

θ – Bragg's angle in degrees,

β – the FWHM in radians.

From the table below, it shows that the crystallite size increases with temperature. It can also be observed that as the deposition temperature increased from 400 to 500 °C, crystallite size increased (See table 5) independently from the deposition time (see Table 5). Crystallite size increases from 1.6 to 36 nm with increasing temperature. The increase of crystallite size may be owing to non-uniform stress or strain during the grain growth or to the existence of local structural disorder in the material [74].

Table 5. Deposition temperature and crystallite size using (200) reflection of orthorhombic SnO_2 thin films.

Deposition Temperature (°C)	Time (min)	Crystallite size (nm)
300	**5**	**2***
	10	**7***
400	**5**	**3**
	10	**5**
500	**5**	**33**
	10	**36**

*** - calculated from (111) reflection of cubic SnO_2**

4.1.2 Optical Properties

The total transmittance spectra of the deposited SnO_2 thin films with different deposition temperature (T_s) recorded at wavelength range 250 to 1500 nm is displayed in Figure 10. All the films exhibit high transmittance in the visible region as well as the IR region. Average transmittance varies between 75 to 80% as deposition temperature increased from 300 to 500 °C. As observed, for temperature 300 and 400 °C, soda lime glass cuts the signal from SnO_2 film in the shorter wavelength region. In the case of 500 °C, band-gap determination difficulties was due to no linear part in Tauc plot. A little shift to the band edge region for higher wavelengths was observed for different deposition times.

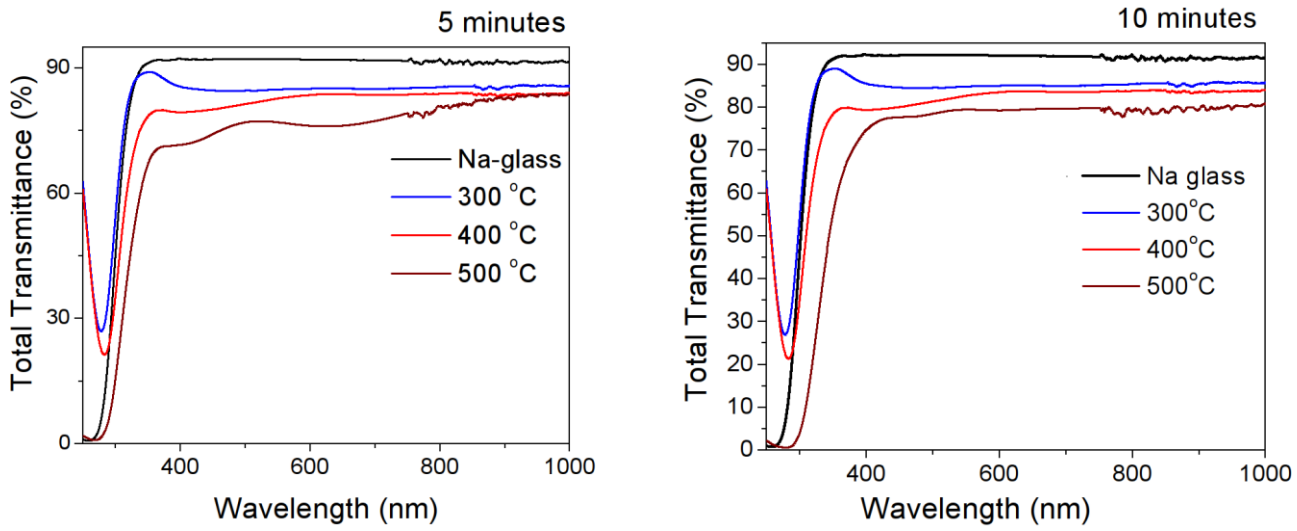

a) b)

Figure 11. Total transmittance spectra of the deposited SnO_2 thin films on glass substrate (a) for 5 min (b) for 10 min.

4.1.3 Thickness of SnO_2 thin films on glass substrate.

The thicknesses of SnO_2 thin films were determined by using peaks and valleys from optical spectrum. This method was first reported by Swanepoel [75]. Usually to calculate the film thickness of a substrate, the total transmittance would be used for the thicknesses measurement of thin films on glass substrates while the total reflectance was selected for the thicknesses measurements of films on substrates. If the refractive index is known, the film thickness can be calculated using the following equation:

$$d = \frac{p}{2\sqrt{n^2 - sin^2\theta}} \times \frac{\lambda_1 \times \lambda_2}{\lambda_1 - \lambda_2} \qquad [5.5]$$

Where

d- film thickness, nm,

n- refractive index,

θ- the angle of incident light,

p- periodicity of interference wave between peak and valley,

$\boldsymbol{\lambda}_1$- the wavelength of peaks, nm,

$\boldsymbol{\lambda}_2$- the wavelength of valleys, nm.

In this study, we determined the thickness of the films by approximation based on peaks and valleys from optical spectrum.

4.1.4 The bandgap of SnO_2 thin films deposited onto glass substrates.

The indirect optical band gap was calculated by using the optical transmittance and reflectance for SnO_2 thin films on glass substrates. To further characterize the optical properties of deposited SnO_2 films, the band gap was calculated using the Tauc relation [37, 76]:

$$a(hv) = B(hv - Eg)^m \qquad [5.6]$$

where

α- the absorption coefficient,

hv- the photon energy, eV,

Eg- the optical band gap, eV,

B- constant, which does not depend on the energy,

m- constant, which characterizes electronic conversion of light absorption. (m=½ for allowed direct transitions, m=2 for allowed indirect transitions).

The transmittance of the thin films is affected by both reflectivity and combination of absorption coefficient and film thickness. The equation [5.7] is used to eliminate the effect of the interference fringes on the transmittance (T) and spectrum [37, 77].

$$\frac{T}{1-R} = e^{-\alpha d} \qquad [5.7]$$

where

α- absorption coefficient,

d- film thickness, nm,

T- total transmittance,

R- total reflectance.

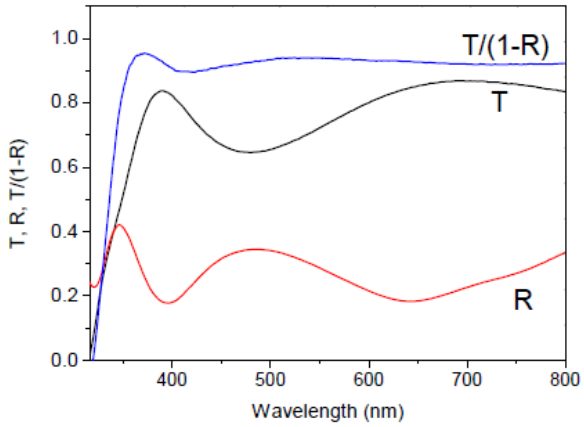

Figure 12. Optical spectrum of $\frac{T}{1-R} = e^{-ad}$ ***(T= transmittance, R= reflectance)*** [37,75]**.**

The direct band gap was assumed for the films on glass substrates, so the equation two can be written as:

$$(a.hv)^2 = B^2(hv - Eg) \qquad [5.8]$$

The optical band gap was obtained by extrapolating the linear part of the plot of $(ahv)^2$against *hv* to the photon energy axis is shown in Figure 13.

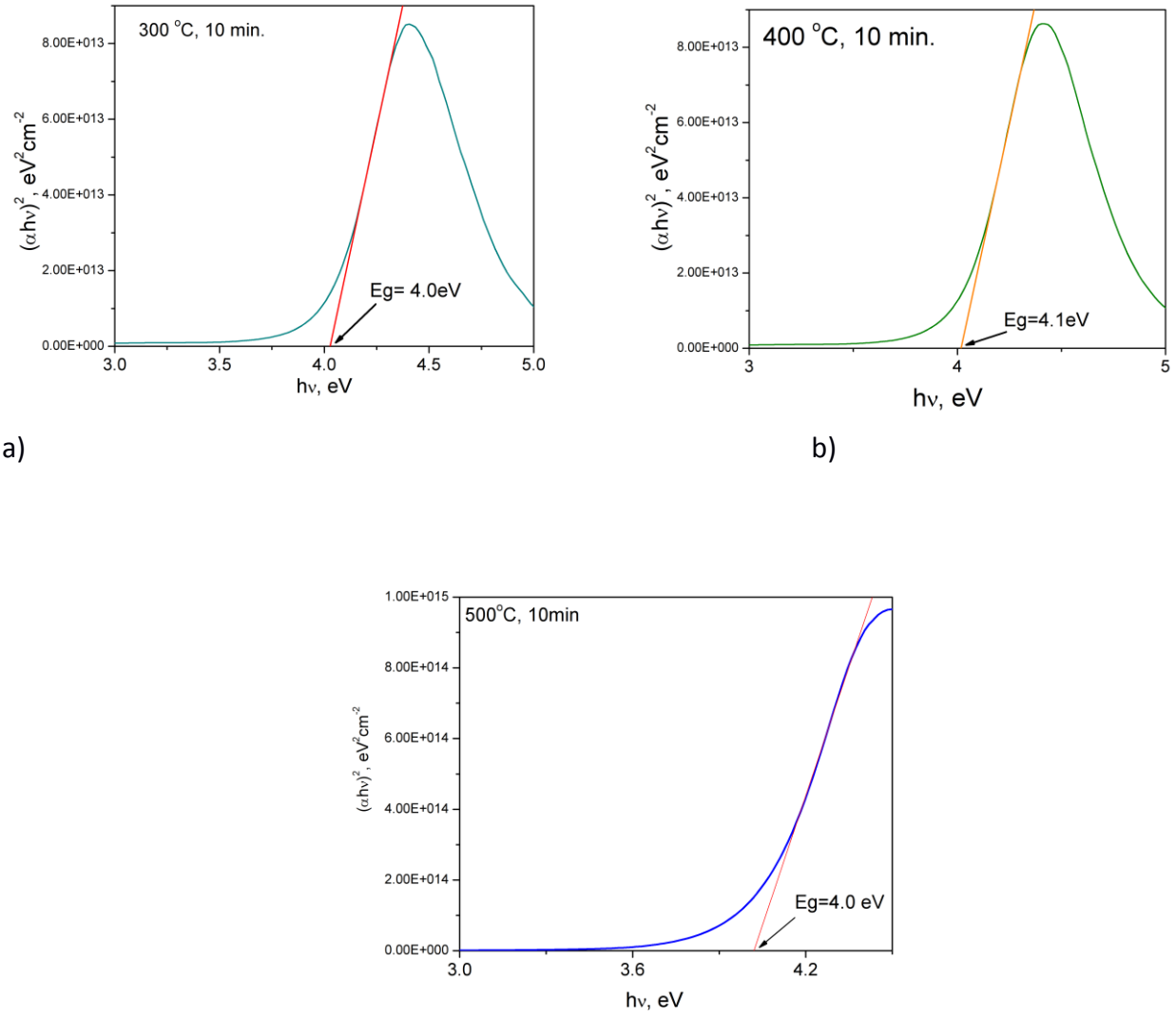

a) b)

c)

Figure 13. Band gap of SnO_2 thin films on glass substrates for a) 300°C b) 400°C b) 500°C

The bandgap for 300 and 500 °C is 4.0 eV while that of 400 °C is 4.1 eV. Rus et al [78] noted that in his study noted that for films with thickness of 55nm and above, the corresponding bandgap is from 4.1 to 4.5 eV.

From figure 20 above, we noticed that the soda lime glass substrates intersect the transmittance signal in the 250 to 300 nm region. In the future, we plan to use quartz substrate to overcome this difficulty.

4.1.5 Electrical properties of TiO_2/SnO_2, ITO/SnO_2, FTO/SnO_2 thin films.

The IV curve of ITO/SnO_2, SnO_2/TiO_2 thin films was measured by applying two graphite contacts with a distance (L= 5 mm) on the top of film as shown in figure 14.

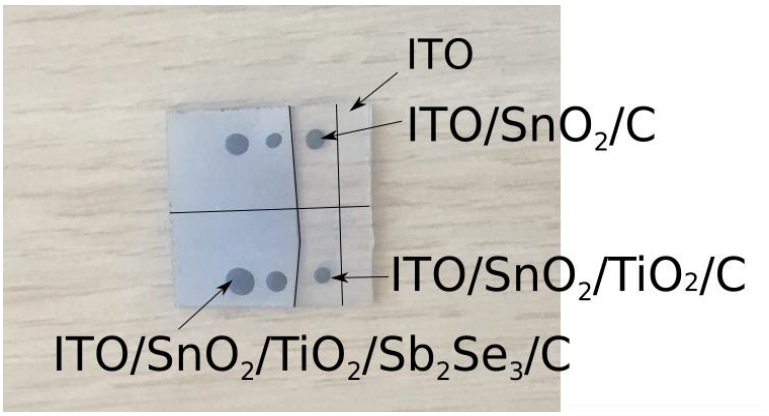

Figure 14. Image of solar cell with contacts on substrate.

The IV measurements were gotten from AUTOLAB PGSTAT 30 system. SnO_2/TiO_2 substrate samples were measured at 400 to 500^{o}C for 10 minutes. A straight line was observed for 500 ^{o}C which indicates an ohmic contact (See figure 15a). An Ohmic contact is a non-rectifying electrical junction that has linear current voltage as with ohm's law. Low resistance ohmic contacts are used to allow charge to flow easily in both directions between the two conductors, without blocking due to or excess power dissipation due to voltage thresholds. Low-resistance, stable ohmic contacts to semiconductors are critical for the performance and reliability of , and their preparation and characterization are major efforts in circuit fabrication. Poorly prepared junctions to semiconductors can easily show rectifying behavior by causing near the junction, rendering the device useless by blocking the flow of charge between those devices and the external circuitry [79] . We could not get any signal for temperature 300 ^{o}C. Figure 15b shows the IV curve of SnO_2 deposited on TiO_2 glass at 300 to 500 ^{o}C for 5 minutes. A non-linear curve was observed. Both materials also appear to be photo sensible.

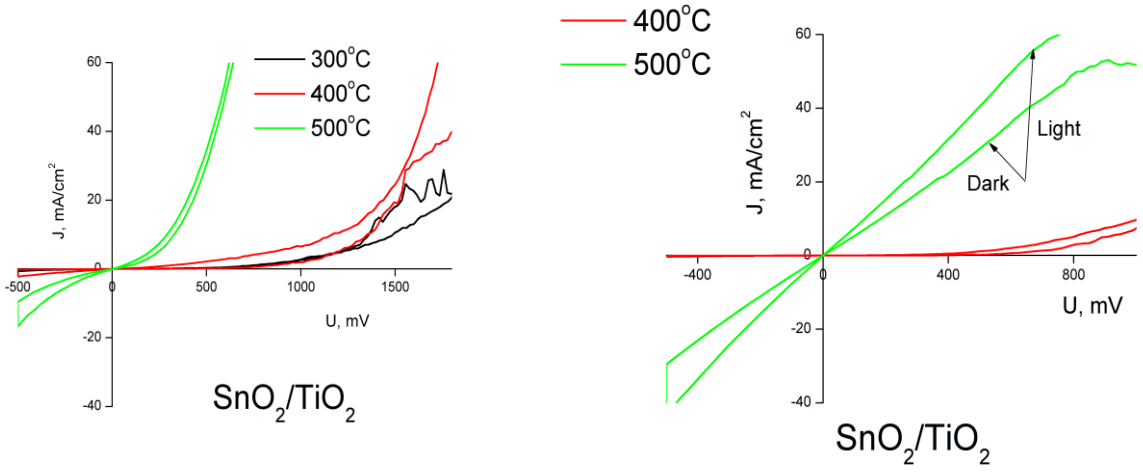

a) ***b)***

Figure 15 a) I-V Curve of SnO_2/TiO_2 for temperature 300 to 500 °C for a) 5 min. and b) for 10 min.

Figure 16 shows the IV curve of SnO_2 deposited on both ITO and FTO substrates. For FTO substrate, even though an ohmic contact is observed, there is little or no change in current density with increasing voltage. While for the ITO substrate, current density increases with voltage favourably at lower temperature. The conductivity of SnO_2 deposited on FTO is not dependent on deposition temperature.

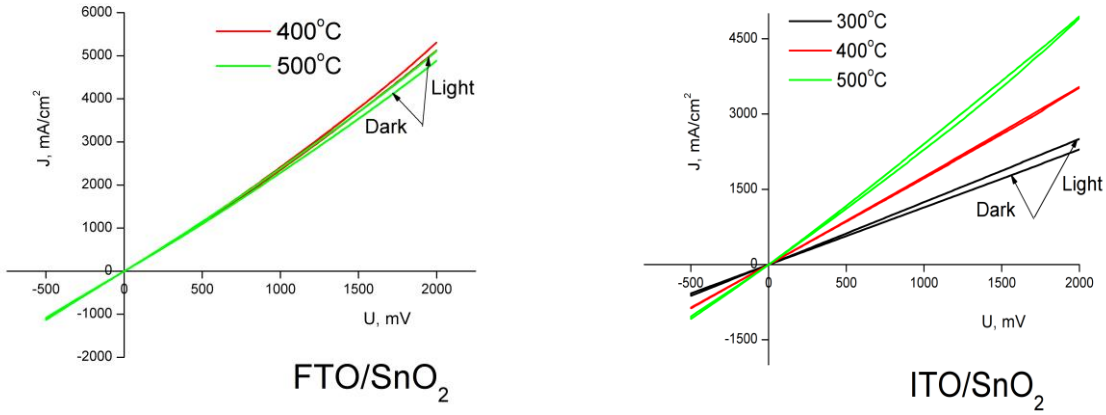

a) **b)**

Figure 16. I-V Curve of a) FTO/SnO_2 and b) ITO/SnO_2 thin films for temperature 300 to 500 °C.

4.1.6. Hall and Van der Pauw

Table 6 shows the variation of resistivity, carrier concentration, hall co-efficient, mobility and sheet resistance of substrates from 300 to 500°C of SnO_2 thin films. Hall Effect measurements were done using the Vander Pauw technique in order to determine the dominant charge carrier type, charge carrier mobility and charge

carrier concentration. It can be seen that the electrical resistivity of the deposited film decreases from 12 Ω•cm to $6.2 \bullet 10^{-3}$ Ω•cm with increase in substrate temperature from 300 to 500^0C. The decrease of electrical resistivity may be due to the increased crystallite size. The charge carrier type was electrons. The density and hall concentration decreased with substrate temperature from 300 to 500 °C while mobility and sheet resistance increase.

Oxygen vacancies and interstitials Sn ions play an important role as charge carriers. Oxygen vacancies can be created by controlling the substrate temperature or ambient oxygen pressure.

Table 6. Density, resistivity, hall co-efficient, mobility, sheet resistance and carriers of SnO_2 thin films on Na-lime glass substrates.

Temperature (°C)	Resistivity Ωcm	Density cm^{-3}	Type of carriers	Sheet resistance $Ω/cm^2$
300	$1.2 \cdot 10^{+1}$	$1.6 \cdot 10^{+18}$	Electrons	$1.2 \cdot 10^{+6}$
400	$9.4 \cdot 10^{-3}$	$3.4 \cdot 10^{+20}$	Electrons	$9.5 \cdot 10^{+2}$
500	$6.2 \cdot 10^{-3}$	$1.0 \cdot 10^{+21}$	Electrons	$6.2 \cdot 10^{+2}$

The electrical resistivity of SnO_2 thin films on glass substrates is presented in Figure 17. It can be observed that the resistivity decreased with increasing the deposition temperature. This could be related to the theory that by increasing the deposition temperature, the quality of crystallite structure become better and the film thickness is increases [77]. The resistivity value is in a range of 10^1-10^{-3} Ωcm which is similar to the values reported by other researchers [9].

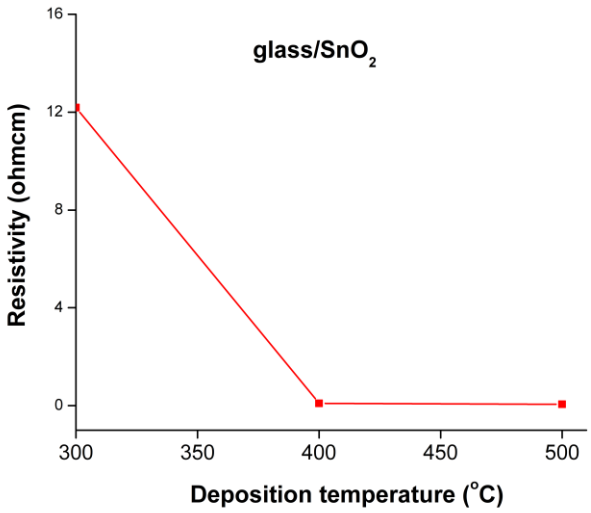

Figure 17. Graph of Resistivity vs Deposition temperature for glass/SnO_2 thin films.

4.1.7. Solar cell properties.

SnO_2 thin films deposited at 300 ^{O}C, 400 ^{O}C, and 500 ^{O}C were tested in a solar cell with structure of glass/ITO/SnO_2/TiO_2/Sb_2Se_3/C. In this structure, ITO is front contact, TiO_2 is window layer, SnO_2 is the interface between window and front contact layer. The test solar cell structure did not consist of an absorber layer. A 3D version of the fabricated solar stack is shown in figure 18.

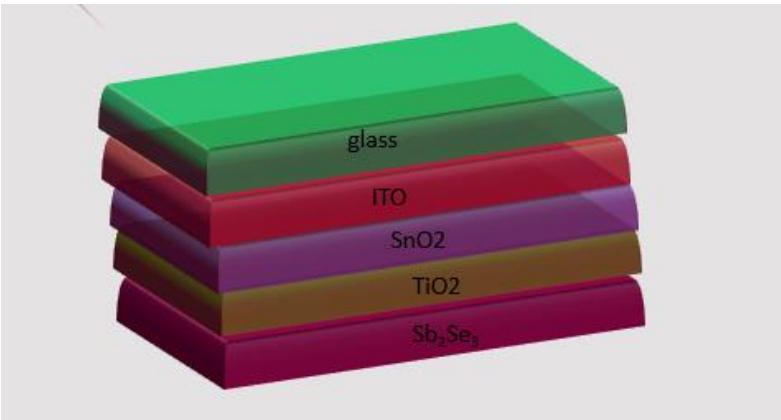

Figure 18. 3d stack of glass/ITO/SnO_2/TiO_2/Sb_2Se_3/C solar cell structure.

The performance of the solar cell was examined using a halogen lamp at an intensity of 100 mW/cm^2. The fill factor and conversion efficiency of the cells were characterized by the following equation below:

$$FF = \frac{I_{max} \times V_{max}}{I_{sc} \times V_{oc}}, \% \qquad [5.9]$$

Where

I_{max}- maximum output of current ,A,

V_{max} - maximum output of voltage, V,

I_{sc} - short-circuit current, A,

V_{oc} - open-circuit voltage, V.

The total energy conversion efficiency was defined as follows:

$$\eta = \frac{I_{SC} \times V_{OC} \times FF}{P_{\text{in}}}, \% \qquad [6.0]$$

Where

I_{sc} - short-circuit current, A,

V_{oc} - open-circuit voltage, V,

FF- fill factor,

P_{in}- intensity of the incident light, w.

Figure 19 shows the I-V curves of SnO_2 solar cells at different deposition temperature. The parameters of the performances of TiO_2 solar cells are as summarized in Table 7. The I-V measurements were performed under the illumination intensity of 100 mw/cm^2, it can be seen from Table 7 that the out-put characteristics of the open circuit voltage (V_{oc}) improved from 0 mV to 317 mV then decreased to 304 mV at 500 ^oC. The short circuit current is very low because of its non-optimized conditions for absorber layer.

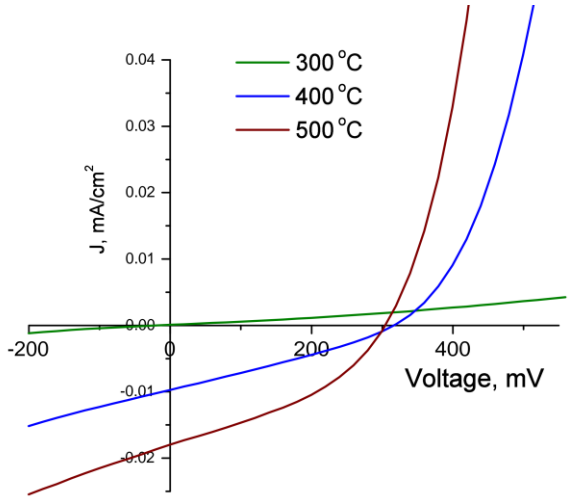

Figure 18. The I-V characteristics of solar cell structure glass/ITO/SnO_2/TiO_2/Sb_2Se_3/C contact, where SnO_2 thin films are deposited by ultrasonic spray pyrolysis at 300 TO 500^oC .

Table 7: Out-put parameters of solar cell structure glass/ITO/SnO_2/TiO_2/Sb2Se3/C where SnO_2 thin films are deposited by ultrasonic spray pyrolysis at 300 to 500^oC.

Temperature (^oC)	Voc (mV)	Jsc (mA/cm^2)	FF (%)	Efficiency (%)
300	0	0	0	0.00
400	317	0.01	31	0.01
500	304	0.02	40	0.01

CHAPTER FIVE

CONCLUSIONS

The main objective of this research is to study the SnO_2 thin films as an interfacial layer for thin film solar cells. SnO_2 acts prevents charge electrical losses at the electrodes thereby prolonging the lifetime and improving the output parameters of the solar cell. SnO_2 was deposited onto glass, ITO or FTO coated glass substrates by ultrasonic spray pyrolysis method. The effect of deposition and time on the structural, optical, electrical properties and the performance of SnO_2 thin films in solar cell with structure of glass/ITO/SnO_2/TiO_2/Sb_2Se_3/C were investigated. They were then characterized by optical measurements, XRD and hot probe.

The key findings obtained from this study are highlighted below:

1) The XRD data reveals that the film at Ts = 300 °C has a cubic structure and orthorhombic crystallization of SnO_2 appears at about 400 °C and above. It was also be observed that as the deposition temperature increased from 400 to 500 °C, crystallite size increased independently from the deposition time from 2 to 33 nm for 5 minutes and from 7 to 36 nm for 10 minutes deposition respectively.

2) For optical properties, all films exhibited high transmittance in the visible region as well as the IR region. Average transmittance varied between 75 to 80% as deposition temperature increased from 300 to 500 ^oC. In the case of sprayed SnO_2 thin films deposited at 300 °C, in shorter wavelength region the soda lime glass could not transmit light and was cut from the spectrum of the SnO_2. A little shift to the band edge region for higher wavelengths was observed for different deposition times for samples deposited at 500 °C. The observed band gap of deposited SnO_2 thin films was between 4.0 and 4.1 eV which corresponded with the literature.

3) Overall, the resistivity and sheet resistance of SnO_2 films was found to decrease with increasing temperature. The resistivity value of films on glass substrate was between 10^3 to 10^{-3} Ωcm. The carrier type was electrons and the density values were found to be between 10^{18} to 10^{21}.

4) The graph of current versus voltage for ITO/SnO_2 and FTO/SnO_2 displayed ohmic behavior at 400 to 500^oC and diode behavior at 300^oC and the conductivity of SnO_2 deposited on FTO is not dependent on deposition temperature. Furthermore, the material was observed to be photo sensible.

5) SnO_2 characteristics can be managed to achieve desirable properties.

6) With further study, undoped SnO_2 can be as an interface between the TiO_2 window layer and ITO layer to prevent electrical losses due to barrier.

RECOMMENDATIONS FOR FUTURE WORK.

It is recommended to produce SnO_2 thin films with different concentrations, spray rate, temperatures and observe how these parameters influences the characteristics of these thin films.

LIST OF REFERENCES

1. BP Statistical Review of World Energy, . June 2013.
2. A review on the utilization of hybrid renewable energy. Renewable and Sustainable Energy Reviews. Volume 91, August 2018, Pages 1121-1147.
3. Renewable energy resources: Current status, future prospects and their enabling technology. Renewable and Sustainable Energy Reviews.
4. Sharker, Komol Kanta et al. “Preparation and Characterization of Tin Oxide based Transparent Conducting Coating for Solar Cell Application.” (2015).
5. T. Söderström, D. Dominé, A. Feltrin, M. Despeisse, F. Meillaud, G. Bugnon, M. Boccard, P. Cuony, F. J. Haug, S. Faÿ, S. Nicolay, C. Ballif. SPIE 7603, 76030B (2010).
6. J. E. Medvedeva and A. J. Freeman. Europhys. Lett, 69 (4), 583–587 (2005).
7. W. Michael, Rowell, A. Mark, Topinka and D. Michael, McGeheea. Appl. Phys. Lett. 88, 233506 (2006).
8. S. Masudat, Y. Kitamura, Okumura, S. Miyatake, H. Tabata, T. Kawai. Transparent thin film transistors using ZnO as an active channel layer and their electric properties J. Appl. Phys., 93 (2003), p. 1624.
9. J. Palanichamy, J.Raj, P. Mohammed, P. Satheesh, S. Kumar, S. Pandiarajan, L. Amalraj. Physical properties of nebulized spray pyrolysised Sno2 thin films at different deposition temperature. Applied physics A [2018] 124:643.
10. A. Goetzberger and C. Helbling. Sol. Energy Mater and solar cells 62, 1 (2000)
11. B. Tosun, Selin & Feist, Rebekah & Campbell, & Aydil, Eray. (2012). Tin dioxide as an alternative window layer for improving the damp-heat stability of copper indium gallium diselenide solar cells. Journal of Vacuum Science and Technology A: Vacuum, Surfaces and Films. 30. 10.1116/1.3692225.
12. Xiong, Liangbin. (2018). Review on the Application of SnO2 in Perovskite Solar Cells.
13. G. Yang, C. Chen, F. Yao, Z. Chen, Z. Zhang, Q .Zheng, X. Ma, J. Lei, H. Qin, P. Xiong, I. Ke, W. Li, G. Yan, Y. Fang. Adv. Mater. 2018, 30, 1706023.
14. Anaraki, H. Kermanpur, A. Steier, l. Domanski, K. Matsui, T. Tress, W. Saliba, M. Abate, A. Grätzel, M. Hagfeldt, A Correa-baena. Energy Environ. Sci. 2016, 9, 3128.
15. Jiang, Q. Chu, Z. Wang, P. Yang, X. Liu, H. Wang, Y. Yin, Z. Wu, J. Zhang, J. You, X Adv. Mater. 2017, 29, 1703852.
16. Thin film solar cell Wikipedia.
17. Mariappan, R. Ponnuswamy, V. Suresh, P. Ashok, N. Jayamurugan, P. Chandra Bose. Superlattices Microstruct. 71, 238–249 (2014)
18. Raj, J. Mohamed, Sanjeeviraja, C. Amalraj. Asian Ceram. Soc. 4, 191–200 (2016).

19. Sehrish, G. Anam, A. Nazmina, I. Saira, R. Shahzad. Tin oxide thin films prepared by sol-gel for PV applications. International Conference on Solid State Physics 2013 (ICSSP'13) Materials Today: Proceedings 2 (2015) 5793 – 5798.
20. Jadsadapattarakul, D. Euvananont, C. Thanachayanont, C. Nukeaw, J. Sooknoi. Tin oxide thin films deposited by ultrasonic spray pyrolysis ceramics international Volume 34, Issue 4, May 2008, Pages 1051-1054.
21. Patil, G. Kajale, Gaikwad, B. and G. H. Jain Spray Pyrolysis Deposition of Nanostructured Tin Oxide Thin Films International Scholarly Research Network ISRN Nanotechnology Volume 2012, Article ID 275872, 5 pages.
22. E. Ramasamy, J. Lee. Ordered mesoporous SnO2-based photoanodes for high-performance dye-sensitized solar cells J. Phys. Chem. C, 114 (2010), pp. 22032-22037.
23. G. Lu, L.E. Ocola, J. Chen. Room-temperature gas sensing based on electron transfer between discrete tin oxide nanocrystals and multiwalled carbon nanotubes Adv. Mater., 21 (2009), pp. 2487-2491.
24. S.S. Pan, C. Ye, X.M. Teng, H.T. Fan, G.H. Li. Preparation and characterization of nitrogen-incorporated SnO2 films Appl. Phys. A, 85 (2006), pp. 21-24.
25. R.E. Presley, C.L. Munsee, C.-H. Park, D. Hong, J.F. Wager, D.A. Keszler. Tin oxide transparent thin-film transistors J. Phys. D, 37 (2004), p. 2810.
26. H. Widjaja, K. Sekizawa, K. Eguchi Low-temperature oxidation of methane over Pd supported on SnO2-based oxides Bull. Chem. Soc. Jpn., 72 (1999), p. 313 , October 2014, Pages 112-255.
27. Soumen Das, V. Jayaraman SnO2: A comprehensive review on structures and gas sensors. Progress in Materials Science, Volume 66, 2014,Pages 112-255,ISSN 0079 6425,https://doi.org/10.1016/j.pmatsci.2014.06.003.
28. T. Minami Transparent conducting oxide semiconductors for transparent electrodes Semi cond Sci Technol, 20 (2005), p. S35.
29. S.R. Vishwakarma, Rahmatullah, H.C.Prasad. Low cost SnO2:P/SiO2/n-Si (textured) heterojunction solar cells J Phys D: Appl Phys, 26 (1993), p. 959
30. M. Batzill, U. Diebold. The surface and materials science of tin oxide Prog Surf Sci, 79 (2005), p. 47.
31. J.E. Medvedeva, A.J. Freeman. Combining high conductivity with complete optical transparency: a band structure approach. Europhys Lett, 69 (2005), p. 583.
32. C. Kiliç, A. Zunger. Origins of coexistence of conductivity and transparency in SnO2. Phys Rev Lett, 88 (2002), p. 095501.
33. L. Gracia, A. Beltrán, J. Andrés. Characterization of the high-pressure structures and phase transformation of SnO2: a density functional theory study. J Phys Chem B, 111 (2007), p. 6479.
34. Baur, W H; Khan, A A Acta Crystallographica B (24,1968-38,1982) (1971) 27, 2133-2139
35. J.E. Hill and R.R. Chamberlin, US Patent 3,148,084 (1964).

36. C. Zengjun. TIO_2 Thin films by ultrasonic spray pyrolysis. Tallinn university of technology School of Engineering Department of Materials and Environmental Technology.
37. R.R. Chamberlein, J.S. Skarman. Chemical spray deposition process for inorganic films, J. Electrochem. Soc., 113 (1) (1966) 86–89.
38. L Filipovic, M Ianeng, S Selberherr, GC Mutinati, E Brunet, S Steinhauer, A Köck, J Teva, J Kraft, J Siegert, F Schrank. Modeling Spray Pyrolysis Deposition, Proceedings of the World Congress on Engineering, 2013, Vol.2.
39. S.P.S. Arya, H.E. Hintermann. Growth of Y-Ba-Cu-O superconducting thin films by ultrasonic spray pyrolysis, Thin Solid Films, 193 (1990) 841–846.
40. H. Yoon, J.H. Woo, Y.M. Ra, S.S. Yoon, H.Y. Kim, S.J. Ahn, J.H. Yun, J. Gwak, K.H. Yoon, S.C. James. Electrostatic spray deposition of copper-indium thin films, Aerosol Sci. Techn., 45 (2011) 1448–1455.
41. P. Svetlana. Tin Sulfide Films by Chemical Spray Pyrolysis: Formation and Properties. Tallinn University of Technology School of Engineering Department of Materials and Environmental Technology.
42. S Pramod. Patil. Versatility of chemical spray pyrolysis technique. Materials Chemistry and Physics, 1999,vol. 59, p. 185-198.
43. MF García-Sánchez, J Peña, A Ortiz, G Santana. Nanostructured YSZ thin films for solid oxide fuel cells deposited by ultrasonic spray pyrolysis. Solid State Ionics, Vol,179, 2008, P. 243-249.
44. E. Leja, J. Korecki, K. Krop and K.Toll 1979 Thin Solid Films vol 59 p 147.
45. A. Czapla, E. Kusior, M. Bucko 1989 Thin Solid Films vol 182 p 15.
46. D. Perednis & J. Ludwig, Gauckler. Thin Film Deposition Using Spray Pyrolysis Nonmetallic Inorganic Materials, Department of Materials, Swiss Federal Institute of Technology, Wolfgang-Pauli-Str. 10, CH-8093 Zurich, Switzerland.
47. C.H. Chen, E.M. Kelder, and J. Schoonman. J.Eur.Ceram.Soc.18, 1439 (1998).
48. V, Vasu & Aryasomayajula, Subrahmanyam. (1990). Electrical and optical properties of sprayed SnO2 films: Dependence on the oxiding agent in the starting material. Thin Solid Films. 193. 973-980. 10.1016/0040-6090(90)90252-9.
49. J.F. Wagner. Transparent electronics Science, 300 (2003), p. 1245.
50. R.L. Hoffman, B.J. Norris, J.F. Wagner. ZnO-based transparent thin-film transistors Appl. Phys. Lett., 82 (2003), p. 733.
51. S. Masuda, K. Kitamura, Y. Okumura, S. Miyatake, H. Tabata, T. Kawai. Transparent thin film transistors using ZnO as an active channel layer and their electric properties. J. Appl. Phys., 93 (2003), p. 1624.
52. R.E. Presley, C.L. Munsee, C.-H. Park, D. Hong, J.F. Wager, D.A. Keszler. Tin oxide transparent thin-film transistors. J. Phys. D, 37 (2004), p. 2810.

53. C.G. Granqvist, A. Hultåker. Transparent and conducting ITO films: new developments and applications. Thin Solid Films, 411 (2002), p. 1.
54. D.R.Deepu et al. How spray rate influences the formation and properties of transparent conducting Sno2 thin films. Journal of analytical physics.
55. A. Dibb, M. Cilense, P. Bueno, R. Aniette, J. Varela, A. Longo (2006). "Evaluation of Rare Earth Oxides doping SnO2.(Co0.25,Mn0.75)O-based Varistor System". Materials Research. 9(3): 339–343. . . 2007-02-10. Archived from on 2012-11-04. Retrieved 2013-03-29.
56. W. . *Acta Crystallographica B (24,1968-38,1982)* (1971) 27, 2133-2139.
57. F. Caillaud, A. Smith, and J.F. Baumard, J. Amer. Ceram. Soc., 76(4), 998 (1993).
58. N.G. Valente, L.E. Cadús, O.F. Gorriz, L.A.Arrúa, J.B. Rivarola. Synergy in Sn–Mo–O catalysts: the selective oxidation of methanol Appl. Catal. A, 153 (1997), p. 119.
59. L.J. Lakshmi, E.C. AlyeaESR. FT-Raman spectroscopic and ethanol partial oxidation studies on MoO3/SnO2catalysts made by metal oxide vapor synthesis Catal. Lett., 59 (1999), p. 73.
60. Chemical sensors, in: T. Seiyama, K. Fueki, J. Shiokawa, S. Suzuki (Jpn Eds.), Proceedings of the International Meeting on Chemical Sensors, held in Fukuoka, Published by Kodansha, Tokyo and Elsevier, Amsterdam, 1983.
61. K. Suito, N. Kawai, Y. Masuda. High pressure synthesis of orthorhombic SnO_2 Mater. Res. Bull., 10 (1975), p. 677.
62. J.M. Mochel, US Patent 2,564,707 (1951).
63. J.E. Hill and R.R. Chamberlin, US Patent 3,148,084 (1964).
64. R.R. Chamberlein, J.S. Skarman. Chemical spray deposition process for inorganic films, J. Electrochem. Soc., 113 (1) (1966) 86–89.
65. J.B. Mooney, S.B. Radding. Spray Pyrolysis Processing, Ann. Rev. Mater. Sci., 12 (1982) 81–101.
66. M. Uurike. Influence of ph on the properties of chemically deposited CDS thin films and solar cells. Tallinn University of Technology School of Engineering Department of Materials and Environmental Technology .
67. H. Yoon, J.H. Woo, Y.M. Ra, S.S. Yoon, H.Y. Kim, S.J. Ahn, J.H. Yun, J. Gwak, K.H. Yoon, S.C. James. Electrostatic spray deposition of copper-indium thin films, Aerosol Sci. Techn., 45 (2011) 1448–1455.
68. D. Perednis & J. Ludwig, G auckler. Thin Film Deposition Using Spray Pyrolysis Nonmetallic Inorganic Materials, Department of Materials, Swiss Federal Institute of Technology, Wolfgang-Pauli-Str. 10, CH-8093 Zurich, Switzerland.
69. M. Okuya, S. Kaneko, K. Hiroshima, I. Yagi, and K. Murakami, J. Eur. Ceram. Soc., 21(10–11), 2099 (2001).
70. H. Gourari, M. Lumbreras, R. Van Landschoot, and J. Schoonman. Sensors and Actuators B, 47(1–3), 189 (1998).

71. M. Jonathan, CdTe solar cells: growth phenomena and device performance, Doctoral thesis, Durham University, 2008.
72. A. Achour Rahal, M. Benhaoua, B. Jlassi, Benhaoua, Superlattices Microstruct. 86, 403–411 (2015).
73. R Swanepoel. Determination of the thickness and optical-constants of amorphous-silicon. J. Phys.E Sci. Instrum. 1983, vol.16, p. 1214–1222.
74. E Houda, M Boujnah, A Taleb. Thickness effect on the optical properties of TiO2-anatase thin films prepared by ultrasonic spray pyrolysis: Experimental and ab initio study. International journal of hydrogen energy, 2017, Vol.42, p. 19467-19480.
75. R. Kykyneshi, DH McIntyre, DHJ Tate, CH Park, DA Keszler. Electrical and optical properties of epitaxial transparent conductive BaCuTeF thin films deposited by pulsed laser deposition. Solid State Sciences, 2008, Vol.10, p. 921-927.
76. S.F. Rus, T.Z. Ward, A. Herklotz, Strain-induced optical band gap variation of SnO2 films, Thin Solid Films, Volume 615, 2016, Pages 103-106, ISSN 0040-6090.
77. MI Khan, S Imran, MS Shahnawaz, UR Saif. Annealing effect on the structural, morphological and electrical. Properties of TiO2/ZnO bilayer thin films. Results in Physics, 2018, vol. 8, p. 249–252.

CYSENI 2019, May 23-24, Kaunas, Lithuania
ISSN 1822-7554, www.cyseni.com

CHARACTERISATION OF SPRAY PYROLYSIS SNO_2 THIN FILMS FOR PHOTOVOLTAIC APPLICATIONS

V. Nwaokolo, A. Katerski

Laboratory of Thin Film Chemical Technologies, Department of Materials Science, Tallinn University of Technology,
Ehitajate tee 5, 19086 Tallinn Estonia.
Phone: +37258779602
Email:crispviv@yahoo.com

ABSTRACT

Due to its unique electronic and optical properties, tin oxide has gained much attention in the field of photovoltaics. This research offers to determine the best conditions for the improvement of component layer in solar cell structure. SnO_2 thin films were synthesized by ultrasonic spray pyrolysis (USP) onto glass substrates at various deposition temperatures (between 300 and 500 °C) using anhydrous $SnCl_4 \cdot 4H_2O$ as a precursor. The films were investigated for structural, optical and electrical properties using X-ray diffraction (XRD), UV-VIS NIR spectrophotometry, hot probe and I-V measurement respectively. All the films display high transmittance in the visible region with average transmittance varying from 75 to 85 %. XRD analysis showed the polycrystalline nature of our samples. Crystallite size increased from 1.6 nm to 36 nm with increasing deposition temperature. Resistivity decreased from $200 \cdot 10^3$ Ohmcm to $78 \cdot 10^3$ Ohmcm with increasing temperature.

Keywords: Thin films, Chemical spray pyrolysis, Spray rate, SnO_2

1. INTRODUCTION

Tin dioxide (SnO_2) has gained much attention in the field of photovoltaics and optoelectronics due to the optical bandgap (3.6 eV), electrical properties (high conductivity and mobility), useful structure, abundance, mechanical hardness, thermal stability in oxidizing environments at high temperature and chemical stability [1, 2]. They are generally regarded as an oxygen deficient n-type oxide semiconductor. Doped with fluorine SnO_2 (FTO) can be used as a transparent conductive oxide in solar cells [3]. This material is more stable and useful for electrode material in solar cells compared to Indium-Tin-Oxide (ITO) [4].

In this paper, we are looking at the various possibilities of using undoped SnO_2 to improve our glass/ITO/TiO_2/SbS_3/back contact solar cell configuration. One of such possibilities is the use of SnO_2 thin films in the window layer (TiO_2) owing to its better optical properties or as an intermediate buffer layer between the ITO/TiO_2 layer of our solar cell [5]. This is because the conductivity of SnO_2 can be easily managed. Additionally, due its useful band structure, high transmittance and stability, they could be used to replace component parts or act as a buffer layer between the front contact electron transport material (ETM) or between the ETM and absorber [6,7]. A broad range of studies has been done in the implementation of SnO_2 thin polycrystalline films in Perovskite solar cells (PSC) [6,7,8,9]. Xiong et al noted a higher efficiency of 20.79% [6]. Hagfeldt and co-workers developed a chemical bath post- treatment SnO_2 PSCs that yielded efficiencies of close to 21%. An impressive certified record efficiency of 20.9% has been achieved by You and co-workers with SnO_2 nanoparticle planar PSCs. Due to this feat, we intend to use SnO_2 to improve our solar cell configuration.

Various types of techniques have been used for the deposition of SnO_2 such as ultrasonic spray pyrolysis (USP) [2, 10], sol-gel method [11], chemical spray pyrolysis [13]. D. Jadsadapattarakul et al reported the microstructure of SnO_2 thin films deposited by ultrasonic spray pyrolysis technique [2]. Sehrish et al investigated the photovoltaic properties of SnO_2 using sol-gel method [11] while S. Palanichamy et al have reported on the physical properties of SnO_2 thin films using nebulised spray pyrolysis [10] at different temperatures. SnO_2 thin films can be deposited using a variety of physical and chemical deposition techniques among which USP is a well-developed and economically viable method for depositing uniform thin films over large area [14]. USP is a processing technique being considered in research to prepare thin and thick films, ceramic coatings, and powders. Unlike many other film deposition techniques, it represents a very simple and relatively cost-effective processing method (especially regarding equipment costs). It offers an extremely easy technique for preparing films of any composition. USP does not require high-quality substrates or chemicals [15, 16].

The aim of this paper is to successfully deposit uniform transparent SnO_2 thin films by USP method onto different substrates (glass and glass/ITO) which are useful for photovoltaic applications and to investigate their structural and electrical properties.

2. EXPERIMENTAL DETAILS

SnO_2 thin films were deposited by ultrasonic spray pyrolysis (USP) technique using an aqueous solution containing 0.1M tin (IV) chloride hydrate (98% Sigma-Aldridge) in 100 ml of pure water (with more than 18 MΩ·cm resistivity). Few drops of hydrochloric acid was added to prevent hydrolysis. To prepare good quality films without contamination, the soda-lime glass and glass/ITO sheets with (10 x 20 x 1 mm) dimensions were cleaned and used as a substrate on which tin oxide thin films were grown. For this experiment, thin films are defined as having 50-100nm thickness.

The experimental setup and detailed discussion of USP technique has already been published [2, 12]. The glass substrates were then sprayed at the rate of 5 l/min for 5 minutes and 10 minutes at temperatures ranging from 300-500 ^oC. Optical measurements was performed by measuring total transmittance and reflectance using Jasco-V670 spectrophotometer in the wavelength range of 250 to 1500 nm. XRD patterns were obtained using ULTIMA IV Rigaku D/Max 2500 diffractometer using a Cu Ka radiation (λ=1.5406 Å, 40 kV at 40 mA). N type conductivity was proved by using hot probe. The value of slope contact behavior and area of contact was obtained from AUTOLAB program while the thickness of the film was determined by optical measurements and used to calculate resistivity.

3. RESULTS AND DISCUSSIONS

3.1. Structural Analysis

The XRD diffraction pattern of SnO_2 thin films deposited for 5 min and 10 min are shown in Fig 2 below. According to XRD pattern, cassiterite (ICDD: 01-077-0448) was detected which revealed the polycrystalline nature of the film having a tetragonal structure. Although, a cubic SnO_2 (ICDD: 01-071-5329) with orientation (111) was also detected for both graphs. No reflection connected to an additional phase was noticed. The film at Ts = 300 °C has an amorphous structure and crystallization of SnO_2 appears at about 400 °C and above. The peak intensity value was substantially raised at 500 °C. It can also be observed that as the

deposition temperature increased from 400 to 500 °C, crystallite size increased independently from the deposition time (see Table 1). The plane (200) appears and was dominant at 500 °C. Similar observation of orientation was reported by Maio et al [18]. Furthermore, a report produced by S. Palanichamy revealed the polycrystalline nature of the SnO_2 thin films and an increase in crystallinity with substrate temperature [2].

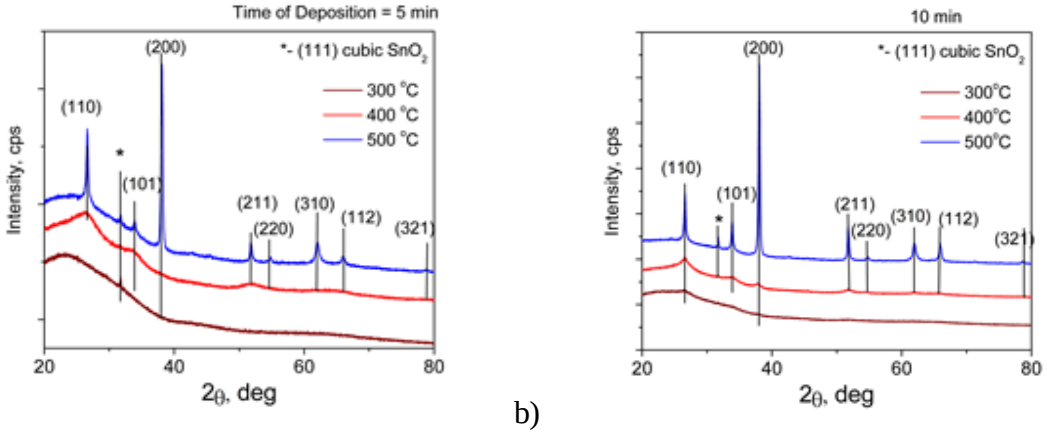

a) b)

Fig. 1.XRD plot of sprayed SnO_2 thin films deposited onto glass substrate (a) for 5min (b) for 10min.

3.2. Optical Properties

The total transmittance spectra of the deposited SnO_2 thin films with different deposition temperature (T_s) recorded at wavelength range 300 to 1500 nm is displayed in Figure 2. All the films exhibit high transmittance in the visible region as well as the IR region. Average transmittance varies between 75 to 80% as deposition temperature increased from 300 to 500 oC. As observed, for temperature 300 and 400 °C, soda lime glass cuts the signal from SnO2 film in the shorter wavelength region. In the case of 500 °C, band-gap determination difficulties was due to no linear part in Tauc plot. A little shift to the band edge region for higher wavelengths was observed for different deposition times.

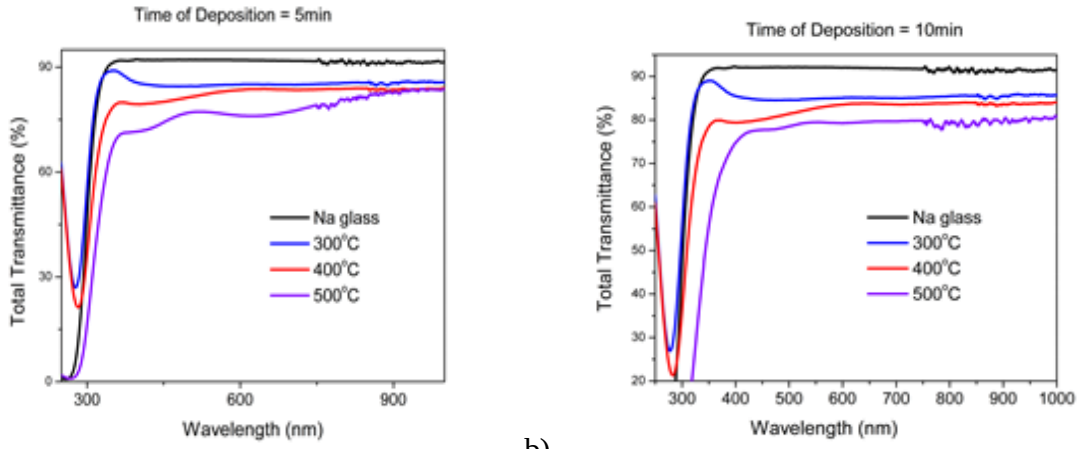

a) b)

Fig. 2. Total transmittance spectra of the deposited SnO_2 thin films on glass substrate (a) for 5 min (b) for 10 min.

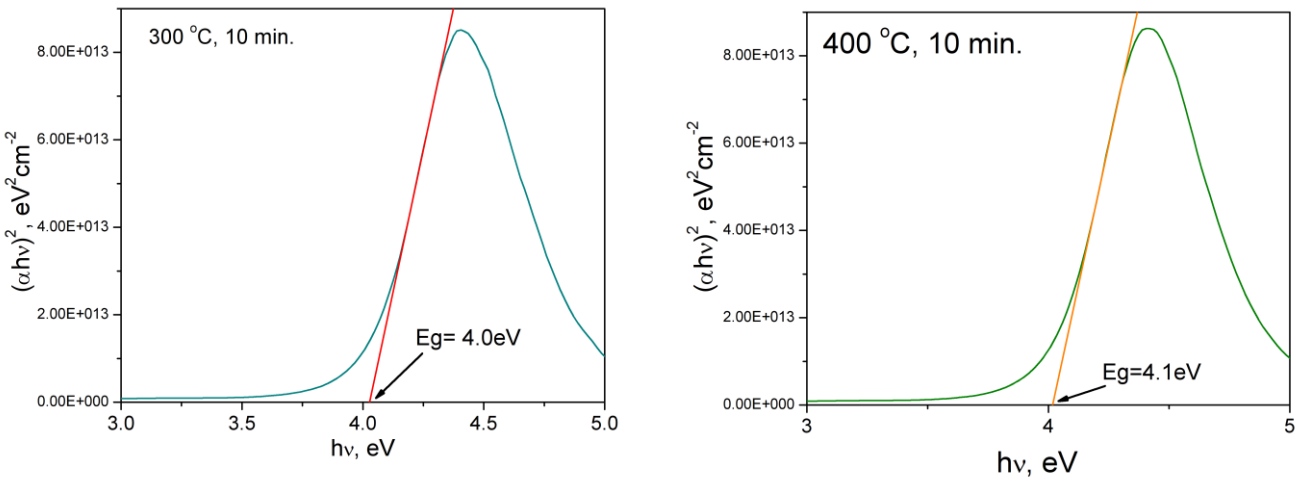

a) b)

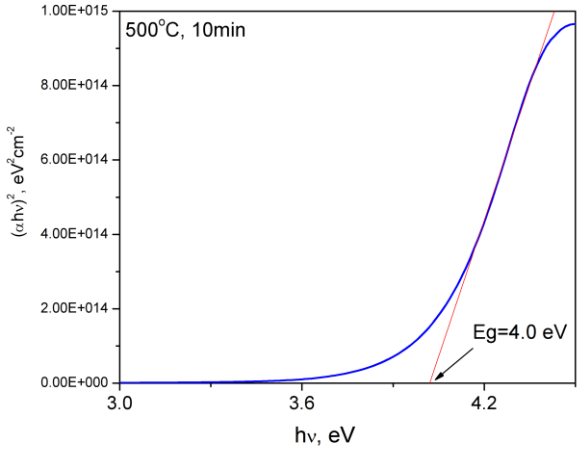

Fig. 3. Band gap of SnO2 thin films on glass substrates for a) 300°C b) 400°C c) 500°C.

The bandgap for 300 and 500 °C is 4.0 eV while that of 400 °C is 4.1 eV. Rus et al [23] noted that in his study noted that for films with thickness of 55nm and above, the corresponding bandgap is from 4.1 to 4.5 eV. From figure 20 above, we noticed that the soda lime glass substrates intersect the transmittance signal in the 250 to 300 nm region. In the future, we plan to use quartz substrate to overcome this difficulty.

3.3. Electrical properties of TiO_2/SnO_2, ITO/SnO_2, FTO/SnO_2 thin films

The IV curve of ITO/SnO_2, SnO_2/TiO_2 thin films was measured by applying two graphite contacts with a distance (L= 5 mm) on the top of film as shown in figure 4. The IV measurements were gotten from AUTOLAB PGSTAT 30 system. SnO_2/TiO_2 substrate samples were measured at 400 to 500°C for 10 minutes.

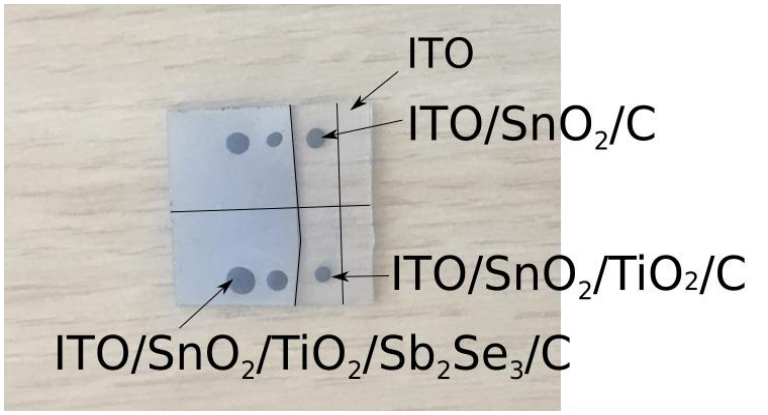

Fig. 4. Image of solar cell with contacts on substrate.

The IV measurements were gotten from AUTOLAB PGSTAT 30 system. SnO_2/TiO_2 substrate samples were measured at 400 to 500ºC for 10 minutes. A straight line was observed for 500ºC which indicates an ohmic contact (See figure 5a). An Ohmic contact is a non-rectifying electrical junction that has linear current voltage as with ohm's law. Low resistance ohmic contacts are used to allow charge to flow easily in both directions between the two conductors, without blocking due to rectification or excess power dissipation due to voltage thresholds. Low-resistance, stable ohmic contacts to semiconductors are critical for the performance and reliability of semiconductor devices, and their preparation and characterization are major efforts in circuit fabrication. Poorly prepared junctions to semiconductors can easily show rectifying behavior by causing depletion of the semiconductor near the junction, rendering the device useless by blocking the flow of charge between those devices and the external circuitry [24] . We could not get any signal for temperature 300 ºC. Figure 5b shows the IV curve of SnO_2 deposited on TiO_2 glass at 300 to 500ºC for 5 minutes. A non-linear curve was observed. Both materials also appear to be photo sensible.

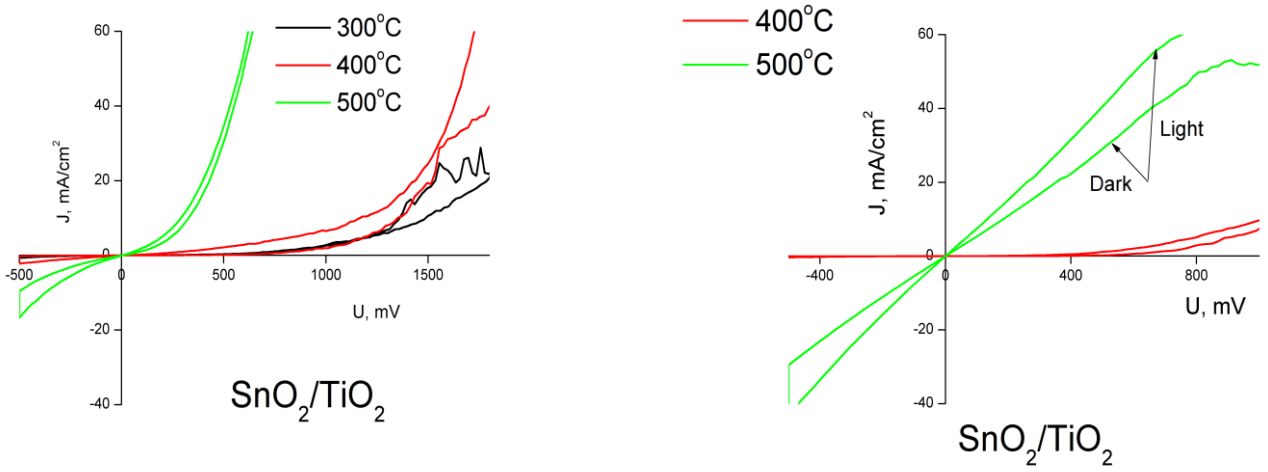

Fig.5. a) I-V curve of SnO2 /TiO2 for temperature 300 to 500oC for a) 5 min. and b) for 10 min.

Figure 6 shows the IV curve of SnO_2 deposited on both ITO and FTO substrates. For FTO substrate, even though an ohmic contact is observed, there is little or no change in current density with increasing voltage. While for the ITO substrate, current density increases with voltage favourably at lower temperature. The conductivity of SnO_2 deposited on FTO is not dependent on deposition temperature.

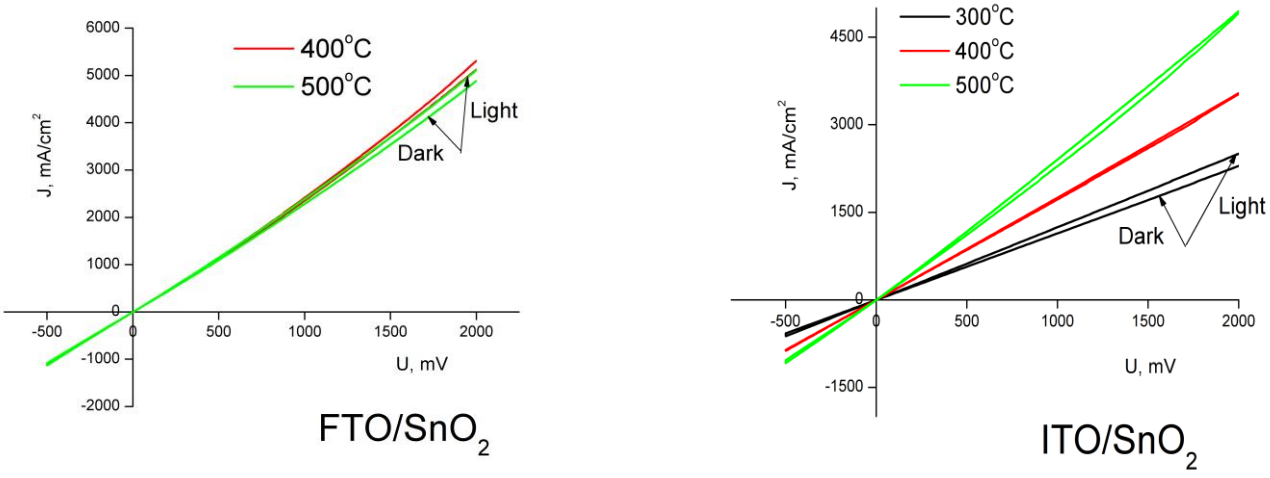

Fig.6. I-V Curve of FTO/SnO2 and ITO/SnO2 thin films for temperature 300 to 500°C.

3.4. Hall and Van der Pauw

Table 1 shows the variation of resistivity, carrier concentration, hall co-efficient, mobility and sheet resistance of substrates from 300 to 500°C of SnO2 thin films. Hall Effect measurements were done using the Vander Pauw technique in order to determine the dominant charge carrier type, charge carrier mobility and charge carrier concentration. It can be seen that the electrical resistivity of the deposited film decreases from 12 Ω•cm to 6.2•10-3 Ω•cm with increase in substrate temperature from 300 to 500^{0}C. The decrease of electrical resistivity may be due to the increased crystallite size. The charge carrier type was electrons. The density and hall concentration decreased with substrate temperature from 300 to 500 °C while mobility and sheet resistance increase.

Oxygen vacancies and interstitials Sn ions play an important role as charge carriers. Oxygen vacancies can be created by controlling the substrate temperature or ambient oxygen pressure.

Table 1. Density, resistivity, hall co-efficient, mobility, sheet resistance and carriers of SnO2 thin films on Na-lime glass substrates.

Temperature (°C)	Resistivity Ωcm	Density cm^{-3}	Type of carriers	Sheet resistance $Ω/cm^2$
300	$1.2 \cdot 10^{+1}$	$1.6 \cdot 10^{+18}$	Electrons	$1.2 \cdot 10^{+6}$
400	$9.4 \cdot 10^{-3}$	$3.4 \cdot 10^{+20}$	Electrons	$9.5 \cdot 10^{+2}$
500	$6.2 \cdot 10^{-3}$	$1.0 \cdot 10^{+21}$	Electrons	$6.2 \cdot 10^{+2}$

The electrical resistivity of SnO_2 thin films on glass substrates is presented in Figure 7. It can be observed that the resistivity decreased with increasing the deposition temperature. This could be related to the theory that by increasing the deposition temperature, the quality of crystallite structure become better and the film thickness is increases [25]. The resistivity value is in a range of 10^{1}-10^{-3} Ωcm which is similar to the values reported by other researchers [2].

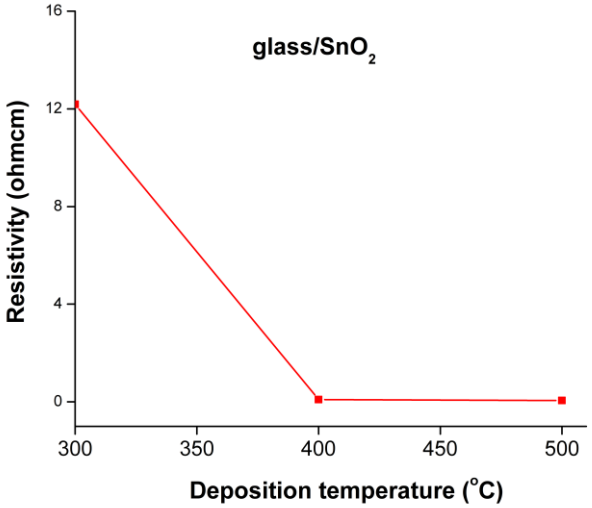

Figure 7. Graph of Resistivity vs Deposition temperature for glass/SnO2 thin films.

3.5. Solar cell properties

SnO2 thin films deposited at 300 OC, 400 OC, and 500 OC were tested in a solar cell with structure of glass/ITO/SnO2/TiO2/Sb2Se3/C. In this structure, ITO is front contact, TiO2 is window layer, SnO2 is the interface between window and front contact layer. The test solar cell structure did not consist of an absorber layer. A 3D version of the fabricated solar stack is shown in figure 8. The performance of the solar cell was examined using a halogen lamp at an intensity of 100 mW/cm^2.

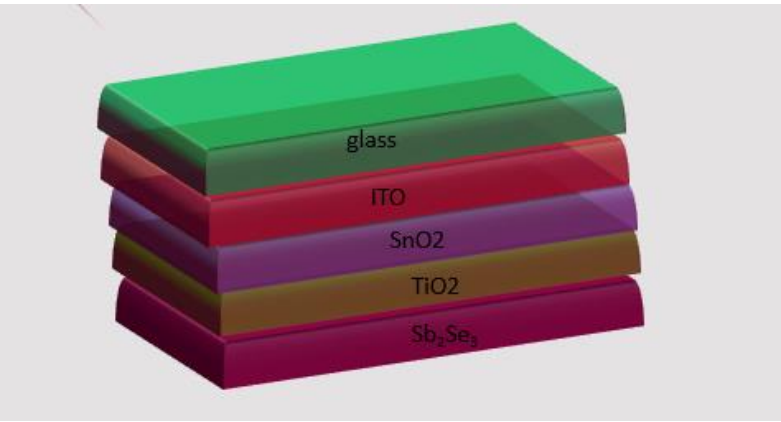

Figure 8. 3d stack of glass/ITO/SnO2/TiO2/Sb2Se3/C solar cell structure.

Figure 9 shows the I-V curves of SnO_2 solar cells at different deposition temperature. The parameters of the performances of TiO_2 solar cells are as summarized in Table 7. The I-V measurements were performed under the illumination intensity of 100 mw/cm^2, it can be seen from Table 7 that the out-put characteristics of the open circuit voltage (V_{oc}) improved from 0 mV to 317 mV then decreased to 304 mV at 500 ^oC. The short circuit current is very low because of its non-optimized conditions for absorber layer.

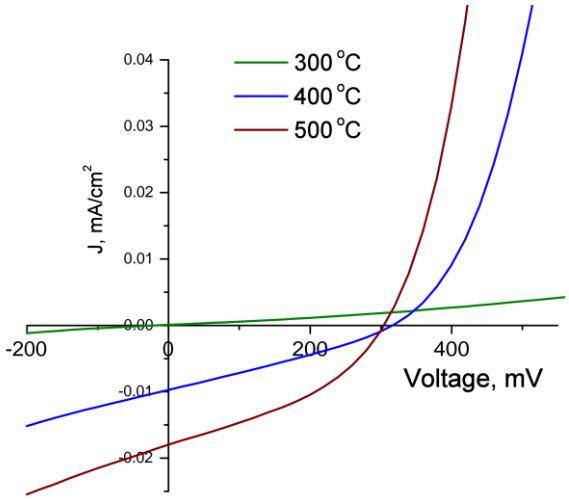

Figure 9. The I-V characteristics of solar cell structure glass/ITO/SnO_2/TiO_2/Sb2Se_3/C contact, where SnO_2 thin films are deposited by ultrasonic spray pyrolysis at 300 TO 500^{O}C.

Table 2. The I-V characteristics of solar cell structure glass/ITO/SnO_2/TiO_2/Sb2Se3/C contact, where SnO_2 thin films are deposited by ultrasonic spray pyrolysis at 300 to 500^{O}C .

Temperature (°C)	Voc (mV)	Jsc (mA/cm^2)	FF (%)	Efficiency (%)
300	**0**	**0**	**0**	**0.00**
400	**317**	**0.01**	**31**	**0.01**
500	**304**	**0.02**	**40**	**0.01**

CONCLUSION

USP method was used to deposit uniform and homogenous SnO_2 thin films. The influence of time and temperature on deposited glass substrate was studied. XRD deposited. SnO_2 thin films showed tetragonal structure at deposition temperatures higher than 400. The thin films deposited at 300 °C displayed amorphous behavior. At T_s = 300°C, crystallite size of films is about 1.6 nm and increases at higher deposition temperature. Additionally, this paper establishes the role of deposition temperature on electrical and optical properties as well as structure of SnO_2 thin films. It was observed that at higher deposition temperatures resistivity decreases. This implies that by using USP method, resistivity can be easily changed

by varying temperature. This could be used to determine best conditions for the improvement of component layer in solar cell structure. All films exhibited high transmittance in the visible region as well as the IR region. Overall, the resistivity and sheet resistance of SnO_2 films was found to decrease with increasing temperature. The resistivity value of films on glass substrate was between 10^3 to 10^{-3} Ωcm. The carrier type was electrons and the density values were found to be between 10^{18} to 10^{21}.

REFERENCES

1. MASUDAT, S. KITAMURA, Y. OKUMURA. MIYATAKE, S. TABATA, H. KAWAI, T. *Transparent thin film transistors using ZnO as an active channel layer and their electric properties* J. Appl. Phys., 93 (2003), p. 1624

2. PALANICHAMY, J.RAJ, J. MOHAMMED, P. SATHEESH, S. KUMAR, PANDIARAJAN, S. AMALRAJ, L. *Physical properties of nebulized spray pyrolysised Sno2 thin films at different deposition temperature. Applied physics* A [2018] 124:643.

3. THIRUMOORTHI, M. THOMAS, J. Asian Ceram. Soc. 4, 124–132 (2016).

4. NGAMSINLAPASATHIAN, SUPACHAI & SREETHAWONG, THAMMANOON & SUZUKI, YOSHIKAZU & YOSHIKAWA, SUSUMU. (2006). *Doubled layered ITO/SnO2 conducting glass for substrate of dye-sensitized solar cells*. Solar Energy Materials and Solar Cells. 90. 2129-2140. 10.1016/j.solmat.2005.12.005.

5. TOSUN, B. SELIN & FEIST, REBEKAH & CAMPBELL, S.A. & AYDIL, ERAY. (2012). *Tin dioxide as an alternative window layer for improving the damp-heat stability of copper indium gallium diselenide solar cells*. Journal of Vacuum Science and Technology A: Vacuum, Surfaces and Films. 30. 10.1116/1.3692225.

6. XIONG, LIANGBIN. (2018). *Review on the Application of SnO2 in Perovskite Solar Cells.*

7. YANG, G. CHEN, C. YAO, F. CHEN, Z. ZHANG, Q. ZHENG, X. MA, J. LEI, H. QIN, P. XIONG, L. KE, W. LI, G. YAN, Y. FANG, G. Adv. Mater. 2018, 30, 1706023.

8. ANARAKI, H. KERMANPUR, A. STEIER, L. DOMANSKI, K. MATSUI, T. TRESS, W. SALIBA, M. ABATE, A. GRÄTZEL, M. HAGFELDT, A CORREA-BAENA, J. Energy Environ. Sci. 2016, 9, 3128.

9. JIANG, Q. CHU, Z. WANG, P. YANG, X. LIU, H. WANG, Y. YIN, Z. WU, J. ZHANG, J. YOU, X Adv. Mater. 2017, 29, 1703852.

10. MARIAPPAN, R. PONNUSWAMY, V. SURESH, P. ASHOK, N. JAYAMURUGAN, P. CHANDRA BOSE, A. *Superlattices Microstruct*. 71, 238–249 (2014)

11. RAJ, J. MOHAMED, SANJEEVIRAJA, C. AMALRAJ, L. Asian Ceram. Soc. **4**, 191–200 (2016).

12. JADSADAPATTARAKUL, D. EUVANANONT, C. THANACHAYANONT, C. NUKEAW, J. SOOKNOI, T. *Tin oxide thin films deposited by ultrasonic spray pyrolysis* ceramics international Volume 34, Issue 4, May 2008, Pages 1051-105.

13. SVETLANA, P. *Tin Sulfide Films by Chemical Spray Pyrolysis*: Formation and Properties TALLINN UNIVERSITY OF TECHNOLOGY School of Engineering Department of Materials and Environmental Technology.

14. SEHRISH, G. ANAM, A. NAZMINA, I. SAIRA, R. SHAHZAD, N. *Tin oxide thin films prepared by sol-gel for PV applications*. International Conference on Solid State Physics 2013 (ICSSP'13) Materials Today: Proceedings 2 (2015) 5793 – 5798.

15. JADSADAPATTARAKUL, D. EUVANANONT, C. THANACHAYANONT, C. NUKEAW, J. SOOKNOI, T. *Tin oxide thin films deposited by ultrasonic spray pyrolysis* ceramics international Volume 34, Issue 4, May 2008, Pages 1051-1054

16. PATIL, G. KAJALE, GAIKWAD, B. and G. H. Jain *Spray Pyrolysis Deposition of Nanostructured Tin Oxide Thin Films* International Scholarly Research Network ISRN Nanotechnology Volume 2012, Article ID 275872, 5 pages.

17. DEEPU, D. & KARTHA, C & VIJAYAKUMAR, K. 2016. *How spray rate influences the formation and properties of transparent conducting SnO2 thin films*. Journal of Analytical and Applied Pyrolysis. 121. 10.1016/j.jaap.2016.06.013.

18. DENGKUI M, QINGNAN Z, SHUO W, ZHENDONG W, XINGLIANG Z, XIUJIAN Z. *Effect of substrate temperature on the crystal growth orientation of SnO2:F thin films spray-deposited on glass substrates,* Journal of Non-Crystalline Solids, Volume 356, Issues 44–49, 2010,06.076.

19. MOCHEL, J.M. US Patent 2,564,707 (1951).

20. HILL, J.E. and CHAMBERLIN, R.R US Patent 3,148,084 (1964).

21. PRAMOD, S. PATIL *thin Film Physics Laboratory, Department of Physics, Shivaji University, Kolhapur 416004, India journal of Technology Education*. Materials Chemistry and Physics Volume 59, Issue 3, 15 June 1999, Pages 185-198.

22. ACHOUR, R. BENHAOUA, M. JLASSI, B. BENHAOUA, *Superlattices* Microstruct. 86, 403–411 (2015).

23. RUS S.F, WARD T.Z, HERKLOTZ A. *Strain-induced optical band gap variation of SnO2* films, Thin Solid Films, Volume 615, 2016, Pages 103-106, ISSN 0040-6090.

24. https://en.wikipedia.org/wiki/Ohmic_contact.

25. KHAN M.I et al *Annealing effect on the structural, morphological and electrical. properties of TiO2/ZnO bilayer thin films*. Results in Physics, 2018, vol. 8, p. 249–252.